BROADENING EFFECTS OF ENERGY SPECTRA IN MODULATION SPECTROSCOPY

Masanori Okuyama

February 1973

Osaka University
Faculty of Engineering Science
Toyonaka, Osaka

BROADENING EFFECTS OF ENERGY SPECTRA IN MODULATION SPECTROSCOPY

Masanori Okuyama

Department of Electrical Engineering

Faculty of Engineering Science

Osaka University, Toyonaka, Osaka

February, 1973

ABSTRACT

Broadening effects of differential energy spectra in modulation spectroscopy have been investigated for one-, two- and three-dimensional crystal on various types of critical points. As modulating external perturbation, electric field, photon energy, critical point energy and broadening factor are considered.

In electric field modulation, two broadening factors due to thermal and electric field effects are taken into account as the Lorentzian convolutions in the electrooptical functions. Variations of the amplitudes in the field induced changes of complex dielectric constants, $\Delta\varepsilon_1$ and $\Delta\varepsilon_2$, with the amount of broadening factors Γ_T and Γ_E are presented for a series of certain realistic parameters. Parametric changes in the broadened electrooptical spectra with the amount of broadening factors are also discussed. Calculated electrooptical functions enable us to compare quantitatively with the spectra measured in the electro-

optical experiments, and considerable agreements between the theory and experimental result are obtained.

A generalized expression of broadened complex dielectric functions near the critical points has been presented as functions of parameters of photon energy $\hbar\omega$, critical point energy $\hbar\omega_g$ and broadening factor Γ. A systematic relationship has been found in differential dielectric functions modulated with energy parameters of ω, ω_g and Γ. By using the relationship, the line shapes of the modulated spectra for any dimensional critical point can be easily figured from a differential function.

Density of states functions for anisotropic crystals were calculated by assuming that the electronic band energy $E(k)=E_0-E_1(\cos k_x + q \cos k_y + r \cos k_z)$, where q and r are continuous anisotropic parameters, and their variations with changing crystal symmetry from one- or two- to three-dimensional crystal are examined. Third derivatives of dielectric spectra with a broadening factor, which can be compared to electrooptical spectra, were calculated as a function of the continuous anisotropic parameter. The same kinds of calculations are extended to the other energy parameter modulated dielectric function. Change of the spectral responce with anisotropic parameters is also examined.

ACKNOWLEDGEMENT

The author would like to appreciate his sincerely thanks to Professors S. Namba and Y. Hamakawa for their kind advices and the critical reading of this thesis.

This work has been done at the Semiconductor Laboratory, Faculty of Engineering Science, Osaka University, Toyonaka, Osaka, under the direction of Professor Y. Hamakawa, and the author wants to express his greatest gratitude to Professor Y. Hamakawa for the constant advice, suggestion and encouragement throughout the course of thesis work.

The author wishes to give his deep acknowledgement to Professors S. Namba, T. Makimoto, K. Fujisawa, T. Sueta and S. Narita for their kind guidance in the course of this study at Osaka University.

The author is much indebted to Dr. T. Nishino for his useful advices and discussions throughout the course of this study.

Usual and enjoyable discussions with colleagues of the Semiconductor Laboratory, especially, Dr. K. Ikeda, Messers. K. Naito, Y. Suzuki, M. Yoshida, T. Yanagida, H. Ogawa and M. Takeda are much appreciated.

The author is grateful to his parents for their endless encouragement and support.

TABLE OF CONTENTS

Page

1. INTRODUCTION

It has been well known that the study of optical properties is one of useful experimental approaches for investigations of the energy band structure of solids. In recent ten years, electro-optical effect in semiconductors has been intensively investigated by use of lock-in technique and recognized as a useful tool for the assignment of fine structures in the band structure parameters. On the other hand, theoretical aspect of the band structure studies has also well developed by an aid of large scale electronic computer on some new approaches of pseudopotential method, k·p method, Fourier expansion method etc. The current interest yielded from these both experimental and theoretical developments has born the study of modulation spectroscopy.[1-3] Modulation spectroscopy is an experimental perturbation method to take changes in the absorption, reflectance or the other optical responce by applying an external perturbation, such as electric field, temperature, incident photon energy or stress. The modulated spectrum obtained has some excellent informations of band parameters including the energy and effective mass of the respective critical point. However if there is some broadening effect e.g. due to electron-phonon interaction, the structure of the measured spectra becomes dim and it is difficult to analyze the experimental results with the theory.

Generally broadening effect in absorption, reflectance or

luminescence spectra is very important because it makes fine structures smooth out. For example, as D-line of sodium is radiated by the transition of electron between two energy levels, the spectra must be a δ-function-like energy dependence, but the measured spectra have a broad energy dependence with a line width. This is attributed to the broadening effect caused by the finite lifetime of electron in the energy level and the motion of sodium atom in the sodium-vapor lamp. Recently as a result of the rapid development of experimental techniques in modulation spectroscopy, the characteristic points in the electronic band structure of solids could be discussed in detail. In order to analyze these informative experimental results quantitatively, the calculations of theoretical spectra taking account of the broadening effects are earnestly desired. In modulation spectroscopy having an external perturbation applied to the sample, an additional broadening may appear in the measured spectra.

The purpose of this thesis is to investigate the broadening effects in modulation spectroscopy, in order to analyze the experimental data precisely and obtain valuable informations about electronic band structure. In electrooptical measurements it has been found by several workers that the spectra do drastically change by large broadening effect. For example, the effect of broadening in electroreflectance spectra of germanium in higher interband transition region is shown in Fig.1.1. Around 2eV it is known that there are an M_1 type critical point and its spin-

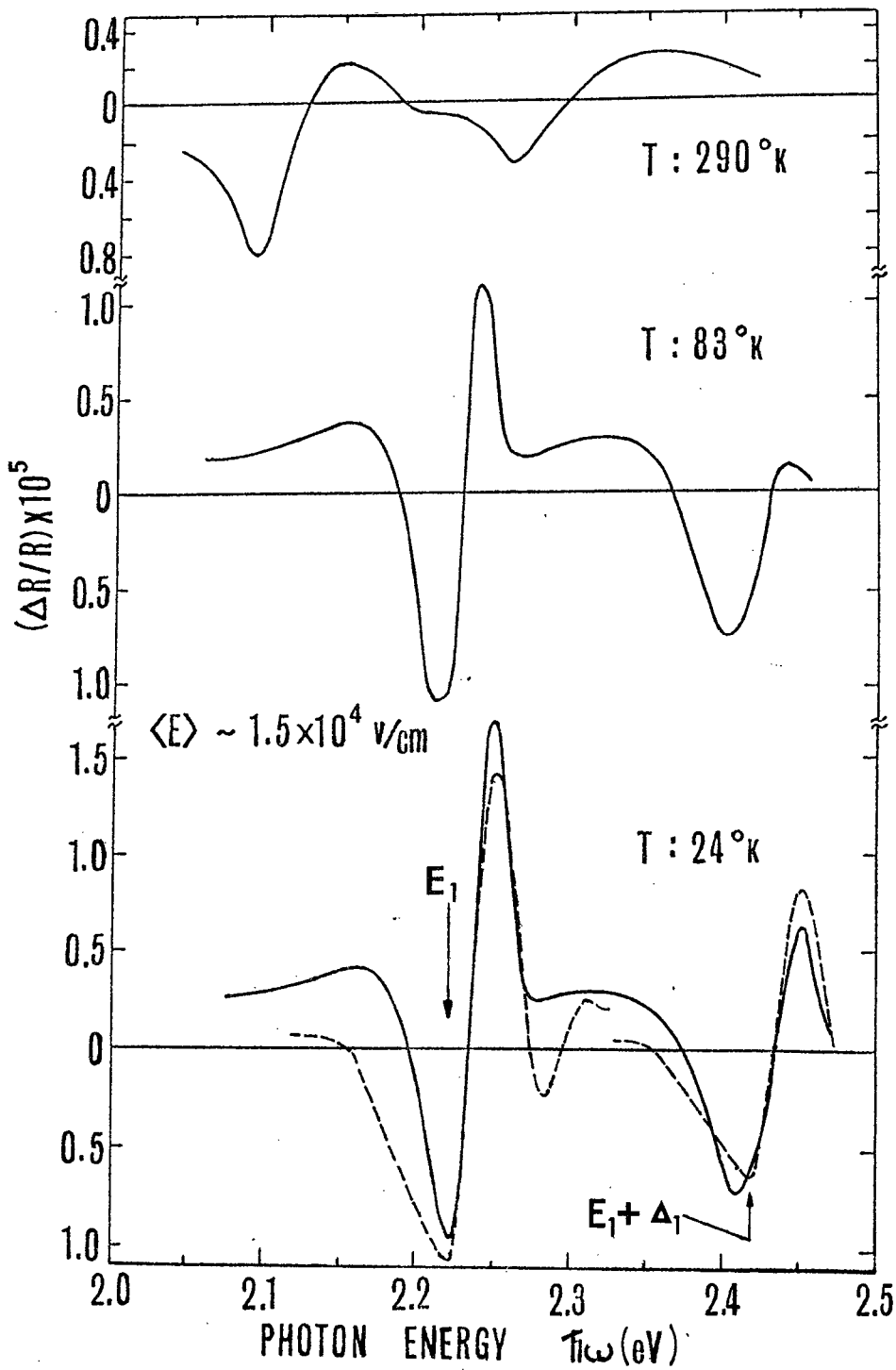

Fig.1.1 Electroreflectance spectra in the energy region 2.0-2.5eV at three different temperature with the same effective electric field[4] (solid line) and the calculated spectra (dashed line).

orbit split edge in germanium. These two critical points have been observed at $\sim$2.2eV(E_1) and $\sim$2.4eV($E_1+\Delta_1$) in the spectrum taken at 24°K. It can be seen in the figure that electroreflectance signal decreases with increasing temperature. And at room temperature characteristic spectrum of M_1 critical point is so much destroyed that E_1 and $E_1+\Delta_1$ signals cannot be distinguished because of large broadening effect. In the case of large broadening which is encountered especially in the higher interband transition region, it is very important to take account of the broadening effects in the analysis of electroreflectance spectra.

In chapter 2 of this thesis, optical properties in solids are simply reviewed to clarify the theoretical background of the results obtained in this work. Modulation spectroscopy is classified into two parts of electric field and energy parameter modulation, and their spectra are derived from the first principle. Chapter 3 describes the studies of the broadening effects in electrooptical signal. The broadening effects in electrooptical signal are classified by the physical sources, and thermal and electric field broadening are the most important in experimentally observed spectra. The electrooptical signals with these broadenings are calculated for some realistic cases and compared with the spectra measured in electroabsorption and electroreflectance.[5] Chapter 4 describes energy parameter modulation spectra for one-, two- and three-dimensional crystals. A generalized expression

of complex dielectric functions is derived[6]. Energy parameter modulation spectra are easily calculated from this generalized expression and summarized by using the relation between these spectra. In chapter 5 modulated spectra in anisotropic crystal such as layer compounds or chain-like crystals are obtained based upon the simple model closer to the realistic crystals. Broadened complex dielectric functions are derived from the calculation of joint density of states for intermediate dimensional band structure. Energy parameter modulation and electrooptical spectra are calculated by the differentiation of the complex dielectric functions.[7] The conlusions of this work are summarized in chapter 6.

References

1. M. Cardona, *Solid State Physics* suppl.11, Ed. by F. Seitz and D. Turnbull (Academic Press, Inc., New York, 1969).
2. B. O. Seraphin, in *Optical Properties of Solids*, Ed. by F. Abeles (North Holland Publishing Co., Amsterdam, 1971) 163ff.
3. B. O. Seraphin et al., in *Semiconductors and Semimetals* vol.9, Ed. by R. K. Willardson and A. C. Beer (Academic Press, New York, 1972).
4. T. Nishino and Y. Hamakawa, J. Phys. Soc. Japan 26, 403 (1969).
5. M. Okuyama, T. Nishino and Y. Hamakawa, Japan. J. Appl. Phys. 7, 1002 (1972).
6. M. Okuyama, T. Nishino and Y. Hamakawa (to be published in J. Phys. Soc. Japan, 1973).
7. M. Okuyama, T. Nishino and Y. Hamakawa (to be published).

2. ENERGY BAND STRUCTURE AND MODULATION SPECTROSCOPY

2.1 Introduction

The study of the optical properties in solids, such as absorption, reflectance or emission of light, has been worked out for the investigations of their electronic band structures. The absorption, reflectance and emission are closely related to the energy band structure of solids through the transitions from one state to another state in the energy band. Hence these optical measurements can be utilized to get some parameters of the energy band structure. The interband transitions can be classified to the direct and indirect in the view of the momentum conservation of electron, and to the allowed and forbidden in the view of the selection rule of momentum matrix element. In this chapter, we have investigated only the direct and allowed transition which is more directly related to the electronic band structure than the others.

2.2 Relation between Optical Constants and Electronic Parameters in Solids

The optical constants in solids[1,2] are characterized by the complex dielectric constant. The refractive index n and the extinction coefficient k are related to the real part ε_1 and imaginary part ε_2 of dielectric constant as follows,

$$\varepsilon_1 = n^2 - k^2 \qquad (2.1)$$

and

$$\varepsilon_2 = 2nk. \tag{2.2}$$

In the absorbing material, the energy of light is reduced at the ratio of $\exp(-\alpha x)$, where α is the absorption coefficient. The absorption coefficient α is related to ε_2,

$$\alpha = \frac{2\omega k}{c} = \frac{\omega}{nc}\varepsilon_2. \tag{2.3}$$

On the other hand, the reflectance is the good probe to investigate the electronic band structure over all the photon energy region, while it is very difficult to measure the absorption spectra in the high energy region above the fundamental edge. In the normal incidence from a vaccum, the intensity reflection coefficient, R, mostly called reflection coefficient is formulated by using Fresnel's formula as follows,

$$R = \frac{(n-1)^2 + k^2}{(n+1)^2 + k^2}. \tag{2.4}$$

A general relationship to connect ε_1 and ε_2 exist and is well known as Kramers-Kronig relations. This dispersion relation is formulated for ε_1 and ε_2,[3)]

$$\varepsilon_1(\omega) = 1 + \frac{2}{\pi} P \int_0^\infty \frac{\omega' \varepsilon_2(\omega')}{\omega'^2 - \omega^2} d\omega \tag{2.5}$$

and

$$\varepsilon_2(\omega) = \frac{2\omega}{\pi} P \int_0^\infty \frac{\varepsilon_1(\omega')}{\omega^2 - \omega'^2} d\omega', \tag{2.6}$$

where P means the Caucy principal part of integration.

From the first perturbation theory, $\varepsilon_2(\omega)$ can be presented for direct interband transition,[2,4]

$$\varepsilon_2(\omega) = \frac{4\pi^2\hbar^2e^2}{m^2\omega^2} \sum_{m,n} \int_{B.Z.} \frac{2}{8\pi^3} d^3k \; |e\cdot M_{fi}|^2 \; \delta(E_{fm}-E_{in}-\hbar\omega) \qquad (2.7)$$

where the summation is over all pair of possible band and the integral is over the first Brillouin zone, and the other notations are the same as in the usual text. Considering the transition between one pair band such as from a valence band to a conduction band and assuming the invariance of the matrix element M_{fi} on wave vector k, the imaginary part of dielectric constant $\varepsilon_2(\omega)$ becomes

$$\varepsilon_2(\omega) = \frac{4\pi^2\hbar^2e^2}{m^2\omega^2} \; |e\cdot M_{cv}|^2 \; N(E), \qquad (2.8)$$

where N(E) is the joint density of states for energy $E=\hbar\omega$,

$$N(E) = \frac{2}{8\pi^3} \int_{E_c-E_v=E} \frac{dS}{|\nabla_k(E_c-E_v)|} \qquad (2.9)$$

and the integral is over the surface of constant energy, $E_c-E_v=E$. The joint density of states, which is proportional to the imaginary part of dielectric constant $\varepsilon_2(\omega)$, has the rapid change in the case of $\nabla_k(E_c-E_v)=0$ from Eq.(2.9). This singular behavior of the joint density of states is called a van Hove's singularity[5] or a critical point in k-space. The energy difference E_c-E_v can be expanded about a critical point of energy difference $E_0(k_0)$ in a Taylor series in effective mass approximation,

$$E_c - E_v = E_0(k_0) + \sum_{i=1}^{N_d} \frac{\hbar^2}{2\mu_i} (k_i - k_{0i})^2 \qquad (2.10)$$

where N_d is the number of dimension of the crystal considered. In three-dimensional crystal, depending on the sign of the reduced effective mass, there are four types of critical points denoted by M_i i=0, 1, 2, 3 where i denotes the number of the negative mass. When the absorption begins from the lowest M_0 critical point, it is well known as the fundamental absorption and has the energy dependence of $(\omega-\omega_0)^{\frac{1}{2}}$. In the case of a two-dimensional k-space which is an appropriate model to treat some aspects of layer structure materials, e.g., graphite and gallium selenide, the density of states N(E) has a step function singularity for the M_0 and M_2 critical point and a logarithmic divergence for M_1 critical point. It is also of interest to mention the energy dependence of a one-dimensional k-space which is appropriate to treat some aspects of chain-like structure materials, e.g., SbSI. For M_0 or M_1 critical point the density of states has the inverse square root singularity.

The behaviors of the optical spectrum near critical points such as edge, peak or step, have been alredy demonstrated both in experimental and theoretical works. Fig.2.1 shows the imaginary part of dielectric constant $\varepsilon_2(\omega)$ of germanium worked out by Brust.[6] The theoretical curve is derived from pseudopotential calculation and the experimental curve is calculated from reflec-

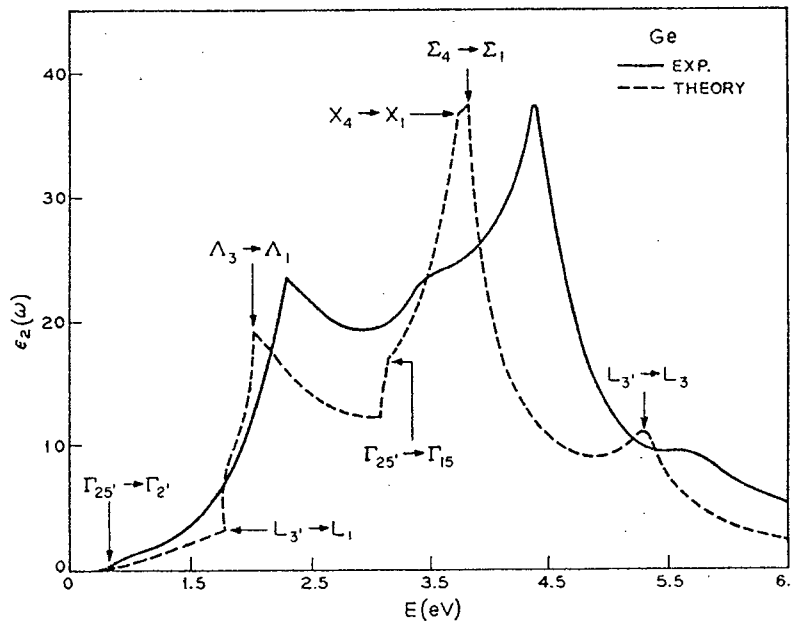

Fig.2,1 Spectral structure of $\varepsilon_2(\omega)$ in germanium. Solid line: experiment ; dashed line:theory, based on pseudopotential energies.(after Brust[6])

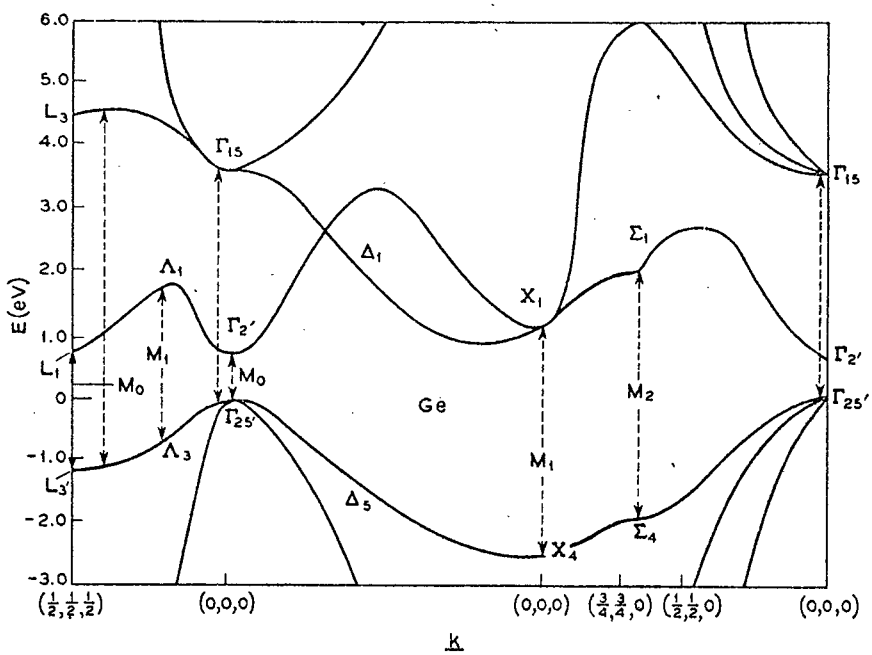

Fig 2,2 The pseudopotential energy bands for germanium along the Brillouin zone. Important direct interband transitions are indicated by arrows.(after Brust[6])

tivity measurement. The dominant peaks and edges have been interpreted as compared with the theoretical considerations. The corresponding pseudopotential energy band for Ge along the principal axes in the Brillouin zone[6] is shown in Fig.2.2. Some important interband transition edges are indicated by arrows and correspond to the singular behavior remarked in Fig.2.1.

2.3 Modulated Spectra of Optical Constants

2.3.1 Introduction

In modulation spectroscopy, the signals are detected as a change of the optical constant by the application of the external perturbation such as electric field, stress, temperature or wavelength of incident light. The resulting spectra are well-resolved and include fine structures than in the conventional method. They are observed only near the critical point and do not contain the background signal observed in the ordinary optical spectra which are the superposition of the spectra caused by some transitions of electron. Modulation spectroscopy can therefore pick up the information about the band structure parameters near critical point. And also it has such advantage that it is possible to analyze the measured spectra by using Kramers-Kronig relation in the small energy region near the critical point.

Modulation spectroscopy can be classified into two categories. The classification is due to the fact whether the external perturbation affects either matrix element or not. The former is electric field modulation or electrooptical effect*, where electric

field changes the matrix element by the deformation of wave function of electron-hole pair. The latters are wavelength, temperature and stress modulation spectroscopy, and we name them energy parameter modulation as their spectra are represented by the dielectric constant differentiated by the energy parameter such as energy of incident light, critical point energy or broadening factor.

2.3.2 Electric Field Induced Changes in Dielectric Constant

Electrooptical effect has been investigated both theoretically and experimentally[7-9] since the earlier calculation of absorption coefficient under uniform electric field by Franz[10] and Keldysh.[11] The theory of electrooptical effect has been extensively developed by many workers, for example, for effective mass approximation by Tharmalingam,[12] for indirect interband transition by Penchina[13] and unified for all kind of critical point by Aspnes.[14,15] Recently the excitonic effects in electrooptical signal have also been studied by several workers.[16-24]

The field induced change in the complex dielectric constants will be derived. According to Dresselhaus'[25] and Elliot's[26] work, the matrix element M_{cv} in Eq.(2.8) is expressed as multiplication of the amplitude of wave function of electron-hole pair in the same unit cell, $\phi(0)$ and the matrix element between the periodic parts of Bloch function, C_0,

$$M_{cv} = \phi(0)\ C_0. \tag{2.11}$$

The wave function of electron-hole pair affected by an electric field can be expressed by using Airy function. For three-dimensional crystal, the imaginary part of dielectric constant near the M_0 critical point can be calculated by using an analytic relationship of Airy function,[27]

$$\varepsilon_{2E}(\omega) = \frac{B\theta^{1/2}}{\omega^2}\,\pi[Ai'^2(\eta) - \eta\, Ai^2(\eta)], \tag{2.12}$$

where

$$B = \frac{2e^2C_0^2}{m^2c\hbar}\left(\frac{8\mu_1\mu_2\mu_3}{\hbar^3}\right)^{1/2},$$

$$\eta = \frac{E_g - \hbar\omega}{\hbar\theta},$$

$$\theta^3 = \frac{e^2E^2}{2\mu_F\hbar},$$

and E_g is band edge energy, E electric field, μ_F the reduced effective mass in the direction of electric field. Thus, the dielectric constant without field $\varepsilon_2(\omega,0)$

$$\varepsilon_{20}(\omega) = \frac{B}{\omega^2}\,(\omega-\omega_g)^{1/2}\,u(\omega-\omega_g) \tag{2.13}$$

where u(x) is the unit step function. One can easily imagine that this expression shows well known square root energy dependence of the dielectric function at the parabolic edge. The field induced change in the dielectric constant, $\Delta\varepsilon_2(\omega)$ is defined as the difference of Eq.(2.12) and (2.13),

$$\Delta\varepsilon_2(\omega) = \varepsilon_{2_E}(\omega) - \varepsilon_{20}(\omega)$$

$$= \frac{B\theta^{1/2}}{\omega^2} F(\eta), \qquad (2.14)$$

where $F(\eta)$ is called the first kind of electrooptical function,

$$F(\eta) = \pi\,[Ai'^2(\eta) - \eta\, Ai^2(\eta)] - (-\eta)^{1/2}\, u(-\eta) \qquad (2.15)$$

and drawn with the solid line in Fig.2.3.

The field induced change in the real part of complex dielectric constant, $\Delta\varepsilon_1(\omega)$ can be obtained through Kramers-Kronig transformation of Eq.(2.5)

$$\Delta\varepsilon_1(\omega) = \frac{B\theta^{1/2}}{\omega^2} G(\eta). \qquad (2.16)$$

$G(\eta)$ is the second kind of electrooptical function,

$$G(\eta) = \pi\,[Ai'(\eta)\, Bi'(\eta) - \eta\, Ai(\eta)\, Bi(\eta)] + \sqrt{\eta}\, u(\eta) \qquad (2.17)$$

and also drawn with the dashed line in Fig.2.3.

It is shown by Aspnes that in the same way, $\Delta\varepsilon_1(\omega)$ and $\Delta\varepsilon_2(\omega)$ for other types of critical points can be expressed by some combinations of the Airy functions, namely the first and second kinds of the electrooptical functions, $F(\eta)$ and $G(\eta)$. Hamakawa et al.[28] have calculated spectra of the dielectric functions, and the line shapes of the field-induced changes of complex dielectric constants at the various critical points for three-dimensional crystals are summarized in Fig.2.4.

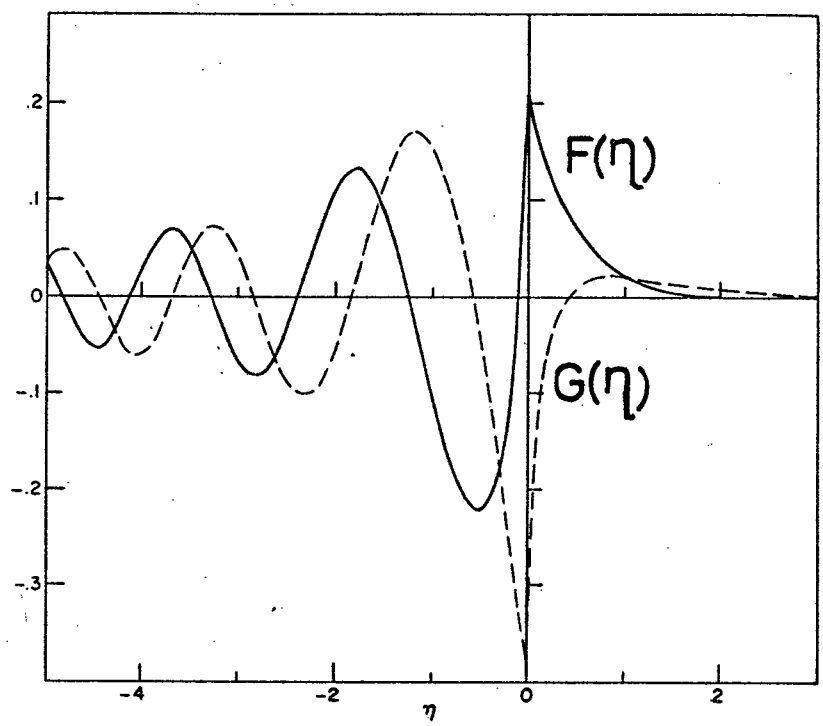

Fig.2.3 Three-dimensional electrooptical functions F(η)(solid line) and G(η)(dashed line).

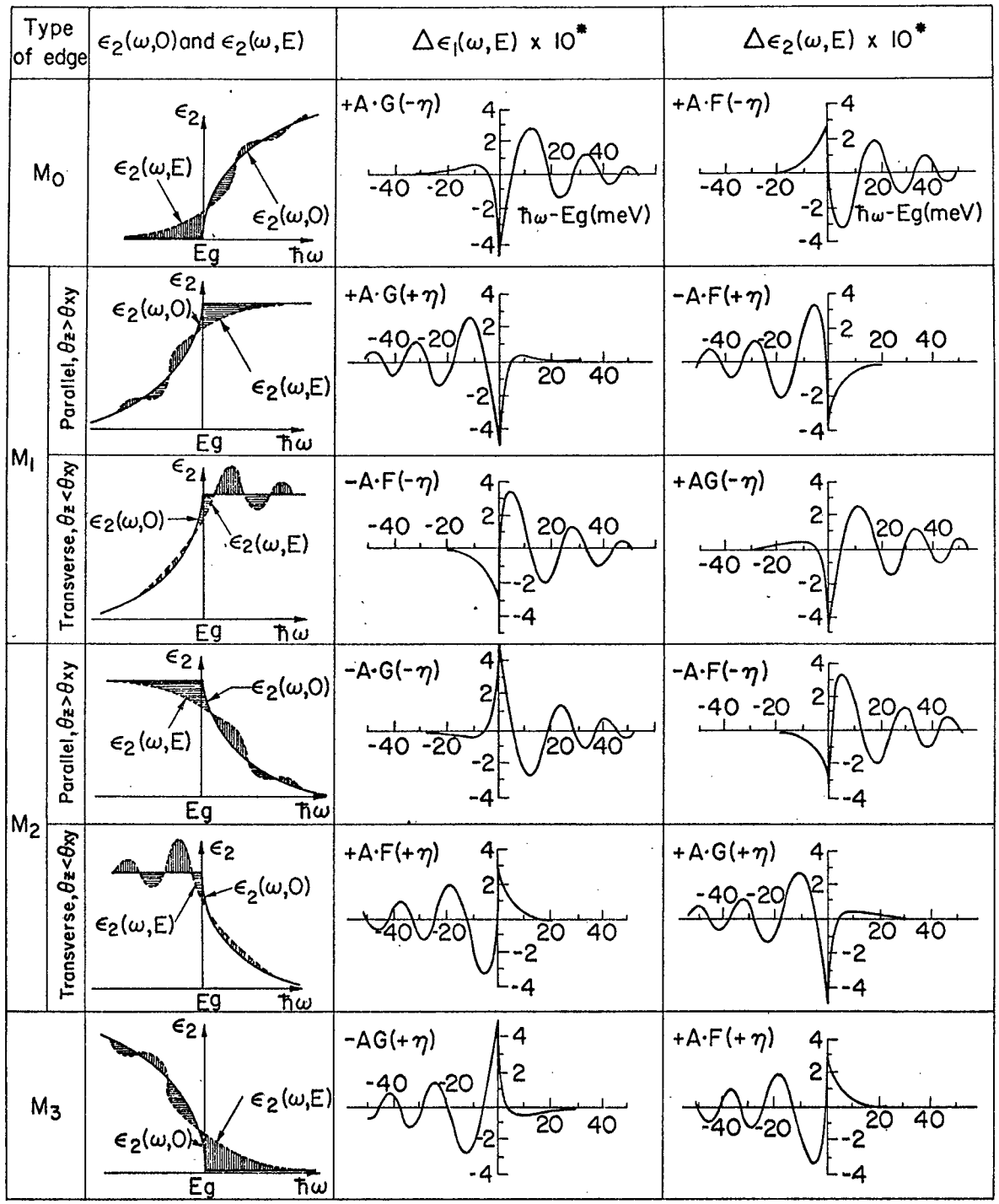

* Line shapes of $\Delta\epsilon_1(\omega,E)$ and $\Delta\epsilon_2(\omega,E)$ calculated at the condition: $\hbar\theta$=10 meV, Eg=0.8 eV and B=1. Here $\eta=(\hbar\omega-Eg)/\hbar\theta$, $A=(B\cdot\theta^{1/2})/\omega^2$

Fig.2.4 A summary of field induced change in the real and imaginry parts of dielectric function at various types of edges.(after Hamakawa et al.[28])

2.3.3 Energy Parameter Modulation in Dielectric Constant

In this section, energy parameter modulated dielectric functions will be derived, as the external perturbations, incident photon energy $\hbar\omega$, critical point energy $\hbar\omega_g$ and broadening factor Γ are considered. Generally the modulated spectra can be expressed by a linear combination of the derivatives of ε_1 and ε_2 with respect to some perturbations.[7,9] In wavelength modulation the complex signal is expressed by the one differentiated with respect to angular frequency of photon, ω,

$$\Delta\varepsilon(\omega) = \frac{d\varepsilon(\omega)}{d\omega}\,\Delta\omega. \tag{2.18}$$

In temperature modulation, the temperature modulated complex dielectric constant is expressed by the differentiated by angular frequency of critical point energy ω_g and broadening factor Γ,

$$\Delta\varepsilon(\omega) = \frac{d\varepsilon(\omega)}{d\omega_g}\frac{d\omega_g}{dT}\,\Delta T + \frac{d\varepsilon(\omega)}{d\Gamma}\frac{d\Gamma}{dT}\,\Delta T. \tag{2.19}$$

$\hbar\frac{d\omega_g}{dT}$ is the temperature coefficient of critical point energy and the absolute value is usually larger than $\frac{d\Gamma}{dT}$. In stress modulation the dielectric constant modulated by hydrostatic pressure is expressed by the derivative with respect to ω_g,

$$\Delta\varepsilon(\omega) = \frac{d\varepsilon(\omega)}{d\omega_g}\frac{d\omega_g}{dP}\,\Delta P. \tag{2.20}$$

In the following chapters we will show detailed spectra of the energy parameter modulation and also discuss their mutual relation-

ships which might be very useful for the analysis of experimental data.[29]

References

1. J. C. Phillips, in *Solid State Physics* 18, Ed. by F. Seitz and D. Turnbull (Academic Press, New York, 1966) 55ff.
2. D. L. Greenaway and G. Harbeke, *Optical Properties and Band Structure of Semiconductors* (Pergamon Press, London, 1968)
3. F. Stern, in *Solid State Physics* 15, Ed. by F. Seitz and D. Turnbull (Academic Press, New York, 1963) 299ff.
4. G. F. Bassni, in *The Optical Properties of Solids*, Ed. by J. Tauc (Academic Press, New York, 1966) 33ff.
5. L. Van Hove, Phys. Rev. 89, 1189 (1953).
6. D. Brust, Phys. Rev. 134, A1337 (1964).
7. M. Cardona, *Solid State Physics* suppl.11, Ed. by F. Seitz, D. Turnbull and H. Ehrenreich (Academic Press, New York, 1969)
8. B. O. Seraphin, in *Optical Properties of Solids*, Ed. by F. Abeles (North Holland Publishing Co., Amsterdam, 1971) 163ff.
9. B. O. Seraphin et al., in *Semiconductors and Semimetals* 9, Ed. by R. K. Willardson and A. C. Beer (Academic Press, New York, 1972).
10. W. Franz, Z. Naturforsch. 139, 484 (1958).
11. L. V. Keldysh, Zh. Eksperim. i Theor. Fiz. 34, 1138 (1958) [Transl.: Soviet Physics-JETP 7, 788 (1958)].
12. K. Tharmalingam, Phys. Rev. 130, 22o7 (1963).
13. C. M. Penchina, Phys. Rev. 138, A924 (1965).
14. D. E. Aspnes, Phys. Rev. 147, 554 (1966).

15. D. E. Aspnes, Phys. Rev. 153, 972 (1967).

16. C. B. Duke and M. E. Alferieff, Phys. Rev. 145, 583 (1966).

17. H. I. Ralph, J. Phys. C 1, 378 (1968).

18. R. Enderlein, Phys. Stat. Sol. 26, 5o9 (1969).

19. C. M. Penchina, J. K. Pribram and J. Sak, Phys. Rev. 188 1240 (1969).

20. D. F. Blossey, Phys. Rev. B 2, 3976 (1970).

21. D. F. Blossey, Phys. Rev. B 3, 1382 (1971).

22. J. D. Dow and D. Redfield, Phys. Rev. B 4, 3358 (1970).

23. J. D. Dow, B. Y. Lao and S. A. Newman, Phys. Rev. B 3, 2571 (1971).

24. B. Y. Lao, J. D. Dow and F. C. Weinstein, Phys. Rev. B 4 4424 (1971).

25. G. Dresselhaus, J. Phys. Chem. Solids 1, 14 (1956).

26. R. J. Elliot, Phys. Rev. 108, 1384 (1957).

27. H. A. Antosiewicz, in *Handbook of Mathematical Functions*, Ed. by M. Abramowitz and I. A. Stegan (U. S. Dept. of Commerce, Natl. Bureau of Standards, Washington, D. C., 1964), Appl. Math. Ser. 55,446ff.

28. Y. Hamakawa, P. Handler and F. A. Germano, Phys. Rev. 167, 709 (1968).

29. M. Okuyama, T. Nishino and Y. Hamakawa (to be published in J. Phys. Soc. Japan, 1973).

* This effect does not include Electrooptic effect, such as Kerr or Pockel effect.

3. THERMAL AND ELECTRIC FIELD BROADENING IN ELECTROOPTICAL EFFECT

3.1 Introduction

A number of investigations on the elctrooptical effect have been recently made for the study of band structure parameters in solids. However, several unresolved problems have been still remained. One of them is an effect of exciton which gives an important role in the low temperature electrooptical effect and this has been studied by several workers[1-6]. Another problem is a broadening effect which is a serious trouble for the quantitative analysis of the electrooptical spectra observed. Especially in the higher interband transition region the effect of broadening is usually dominated by a shortening of the life time of electron and also a spacial inhomogenity by reduction of the penetration depth of photon. Sometimes an overlapping of the signals coming from adjacent critical point destroys its own line shape of the respective edges. In a recent year, a great progress in the band structure studies by the use of computer calculations, and on the other hand experimentally, improvement of the resolutions with the modulation technique makes a study of broadening effect one of the required work in the modulation spectroscory. There has been only a few works concerned in this problem so far. The effect of life time broadening on the electrooptical functions has been demonstrated first by Seraphin[7]. Hamakawa et al.[8] have pointed out that there is another broadening effect

depending upon electric field. Aspnes[9] has derived a general expression of electrooptical functions with the convolution of Lorentzian type broadening effect. Enderlein[10,11] has also calculated the broadened electrooptical spectra. Quite recently Forman et al.[12] has analyzed the data of transverse electroreflectance of GaAs near the fundamental edge in terms of thermally broadened electrooptical spectra. However there has been no work demonstrating the systematic treatment of both thermal and electric field broadening which might be very useful for the analysis of the electrooptical spectra observed.

In this chapter we have calculated the Lorentzian convolutions in the electrooptical functions by taking account of two broadening factors due to thermal and electric field broadenings.[13] A feature of the parametric changes in the broadened electrooptical functions with two broadening factors is examined. We have also obtained a consistent relationship between the calculated results and the experimental data taken at a series of combined conditions. The physical sources of the broadening effects are also discussed.

3.2 Broadening Effect in Electrooptical Signal

As it can be seen elsewhere, the optical spectra observed by experiments are usually much smoother than those expected from the theory. For example, Fig.3.1 shows the temperature dependences of the electroabsorption signals near $\Gamma_{25}'-\Gamma_2'$ transition edge of germanium. The life time broadening is the most familiar source

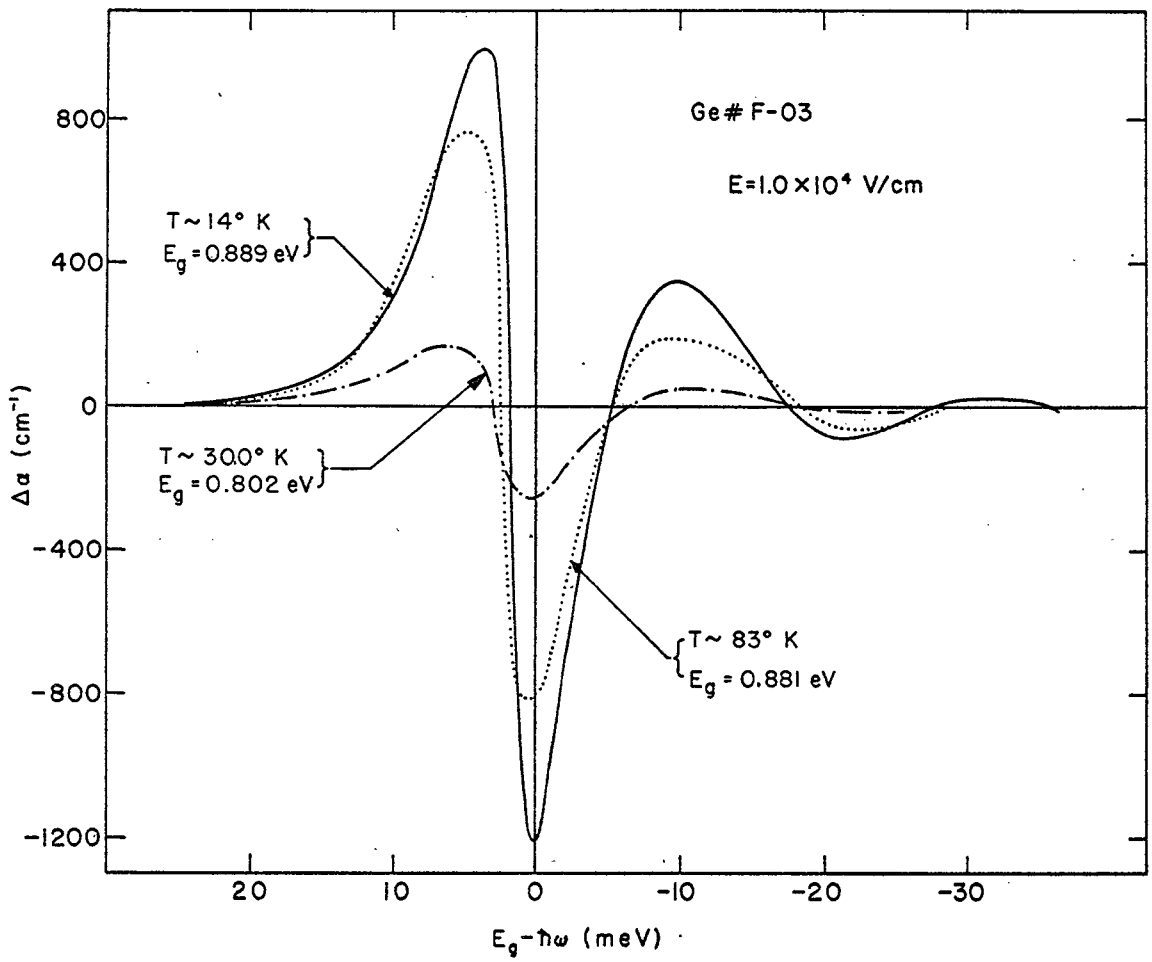

Fig.3.1 The example of thermal broadening effect in electroabsorption in $\Gamma_{25}'-\Gamma_2'$ transition edge of germanium.(after Hamakawa, Germano and Handler[8])

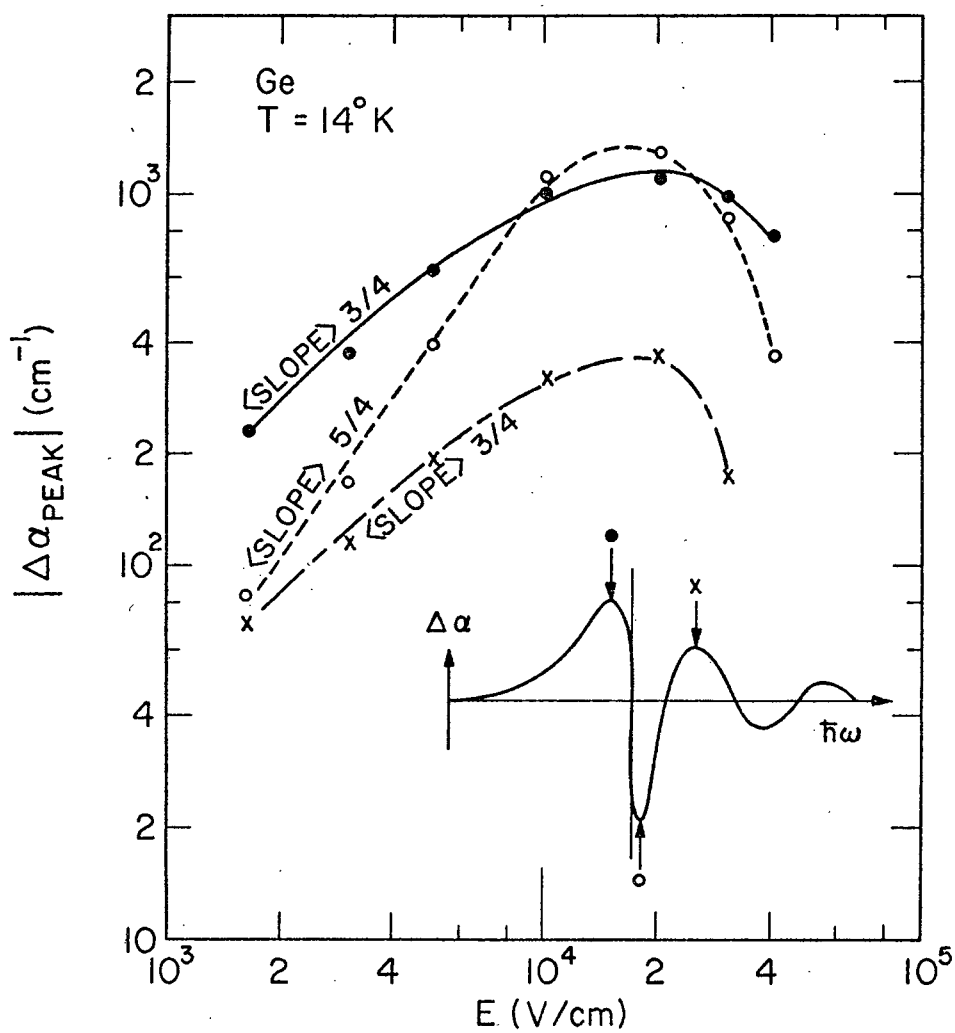

Fig.3.2 The amplitude dependence of the first two positive and first negative peak as a function of the magnitude of the electric field.(after Hamakawa, Germano and Handler[8])

to be considered and intensively investigated for various optical spectroscopy. In the electrooptical effect, however, there are some additional sources resulting from the application of high electric field. At first, we have tried to enumerate possible sources for the broadening effect in the electrooptical spectra as following;

a) thermal broadening, (that is, life time broadening)

b) broadening due to the spacial field inhomogenity,

c) broadening due to the chronological field inhomogenity,

d) electric field broadening arisen from other high field effects.

Thermal broadening effect in the electrooptical signal has been demonstrated first by Seraphin and Bottka[7], Enderlein[10,11] and Forman et al.[12] In a recent year the effect of spacial inhomogenity of electroreflectance signal has been studied by some workers.[13-16] It has been shown that it is avoidable by a careful sample preparation and the electrode alignment to get uniform field on the sample and also in some case that this spacial inhomogenity can be reduced by a proper choice of impurity concentration for a certain electric field applied in the case of surface barrier electroreflectance[17]. Chronological inhomogenity of electric field applied also gives broadening in the electrooptical signal as a time averaging effect. This kind of broadening appears, forexample, in the case of measurements with a sinusoidal electric field modulation. This broadening could be eliminated by using the square wave pulse modulation field having the duration larger

enough than the relaxation time. A drastical change in the electroreflectance line shape has been observed in lead salts by Aspnes and Cardona[18]. This change has been explained by the relaxation time effect in electric field applied across the sample. There is still remained broadening effect in the electrooptical signals. The experimental data show that the electric field dependence of the amplitude in the electrooptical signal does not follow the $E^{1/3}$ law as expected by the theory. The slope of $\log\Delta\alpha$ vs. log E, for example, in the Fig.3.2 shows more than unity in the low electric field region, and decreases gradually with increasing electric field, and eventually changes its sign at certain high electric field. This behavior cannot be interpreted by any broadening sources mentioned above a)∿c). The cause of the broadening might be based upon an effect of high electric field on the electronic states for optical transitions. Then we call this source an electric field broadening.

3.3 Broadened Electrooptical Functions in Three-dimensional Crystal

3.3.1 Derivations of Γ_T and Γ_E

According to the theory of the electrooptical effect in the absence of Coulomb interaction, the field induced change in the real and imaginary part of complex dielectric constant in the interband transition near the critical point of the energy band, $\Delta\varepsilon_1$ and $\Delta\varepsilon_2$, can be expressed by the first and second electro-optical function from chapter 2,

$$\Delta\varepsilon_i(\omega) = \pm \frac{B\theta^{1/2}}{\omega^2} \begin{cases} F(\eta) \\ G(\eta) \end{cases} \qquad i=1,2 \qquad (3.1)$$

where B, θ and η are same as that defined in section2.2. The signs of η and $\Delta\varepsilon_i(\omega)$ are determined by the type of respective critical point.

In order to examine the effect of broadening on electro-optical functions, we have taken two different broadening factors Γ_T and Γ_E in the Lorentzian convolution integral, where Γ_T means the thermal broadening and Γ_E the electric field broadening factor. The broadened spectrum of the field induced change in the imaginary part of dielectric constant, $\{\Delta\varepsilon_2(\omega,\Gamma_T,\Gamma_E)\}_{broad}$ can be calculated by the form,

$$\{\Delta\varepsilon_2(\omega,\Gamma_T,\Gamma_E)\}_{broad} = \{\varepsilon_{2E}(\omega,\Gamma_T+\Gamma_E)\}_{broad} - \{\varepsilon_{2O}(\omega,\Gamma_T)\}_{broad} , \qquad (3.2)$$

where the Lorentzian convolution of a function $F(\omega)$ is generally defined as;

$$\{F(\omega,\Gamma)\}_{broad} = \frac{\Gamma}{\pi}\int_{-\infty}^{\infty} \frac{F(\omega')}{(\omega'-\omega)^2+\Gamma^2}\, d\omega' \cdot \qquad (3.3)$$

As it can be seen from Eq.(3.1) that in the electrooptical function we usually employ a normalized energy scale η, one can also convert the broadening factor Γ into the dimensionless expression of Γ_{TN} and Γ_{EN} having the same unit of η. Inserting the Airy function expression of the imaginary part of dielectric constants with and without electric field into Eq.(3.2), we can calculate

$\{\Delta\varepsilon_2(\omega,\Gamma_T,\Gamma_E)\}_{broad}$ at M_0 critical point by the form;

$$\{\Delta\varepsilon_2(\omega,\Gamma_T,\Gamma_E)\}_{broad} = \frac{B\theta^{1/2}}{\omega^2}\Big[\frac{\Gamma_{TN}+\Gamma_{EN}}{\pi}\int_{-\infty}^{\infty}\frac{Ai'^2(\eta')-\eta' Ai^2(\eta')}{(\eta'-\eta)^2+(\Gamma_{TN}+\Gamma_{EN})^2}\,d\eta' - \frac{\Gamma_{TN}}{\pi}\int_{-\infty}^{\infty}\frac{\sqrt{-\eta'}\,u(-\eta')}{(\eta'-\eta)^2+\Gamma^2}\,d\eta'\Big]. \qquad (3.4)$$

The analytic function of Eq.(3.4) is given by Aspnes[9] using complex Airy functions. It may be assumed that the coefficient $\frac{B\theta^{1/2}}{\omega^2}$ in front of $F(\eta)$ or $G(\eta)$ can be taken away from the integrand Eq.(3.3) because it does only slightly depend upon temperature through the reduced effective mass, the momentum matrix element and angular frequency in the region integrated. Therefore we normalize the dielectric constant by the factor $B\theta^{1/2}/\omega^2$ and calculate the broadening effect on the electrooptical functions to be applicable at any critical point for both electroabsorption and electroreflectance , not in form of $\Delta\varepsilon$. The first and second kind of broadened electrooptical function are designated as $F(\eta, \Gamma_{TN},\Gamma_{EN})$ and $G(\eta, \Gamma_{TN},\Gamma_{EN})$.

3.3.2 Temperature Dependence

First of all, we will consider only the thermal broadening effect. The typical curves of the thermally broadened electrooptical functions, $F(\eta,\Gamma_{TN},0)$ and $G(\eta,\Gamma_{TN},0)$, are shown in Fig.3.3, when Γ_{TN} is changed from 0 to 1.0. The solid line is the one without the broadening which is the original function, $F(\eta)$ or

$G(\eta)$. As shown in these figures, the spike at $\eta=0$ corresponding to the critical point, is rounded off and the other peaks in oscillations at $\eta<0$ are gradually damping with the increase of Γ_{TN} as already pointed out. In the spectra of $F(\eta,\Gamma_{TN},0)$ the peak 1 following the exponential tail shifts far from the position of $\eta=0$ with increasing of Γ_{TN}, and at $\Gamma_{TN}\simeq 0.5$ the shift of this peak attains to more than 0.5 in $\hbar\theta$ unit. As to $G(\eta,\Gamma_{TN},0)$, on the other hand, the peak 1 moves slightly to the negative η side and when the broadening factor Γ_{TN} attains to about 1.0, it does inversely shift to the positive η side. It should be noticed that the other positions do not almost change with Γ_{TN}. Thus, the introduction of these thermal broadenings gives the electro-optical function the effects to round off the spike at $\eta=0$ and damp the other peaks.

The broadened electrooptical functions including an additional electric field broadening can be also calculated by Eq.(3.4). These spectra of $F(\eta,\Gamma_{TN},\Gamma_{EN})$ and $G(\eta,\Gamma_{TN},\Gamma_{EN})$ are shown in Fig.3.4. The parameter Γ_{TN} is fixed at 0.1 and another parameter Γ_{EN} is changed from 0 to 0.1. The variation of Γ_{EN} indicates the various steps of the electric field effect and so this figure does not directly correspond to Fig.3.3. It can be seen in the figure that for $F(\eta,\Gamma_{TN},\Gamma_{EN})$ the peak 1 increases with the electric field broadening and the amplitudes of the other oscillation peaks become small, and for $G(\eta,\Gamma_{TN},\Gamma_{EN})$ the negative peak 1 becomes greater and the other peaks decrease. In Fig.3.5 the dependences

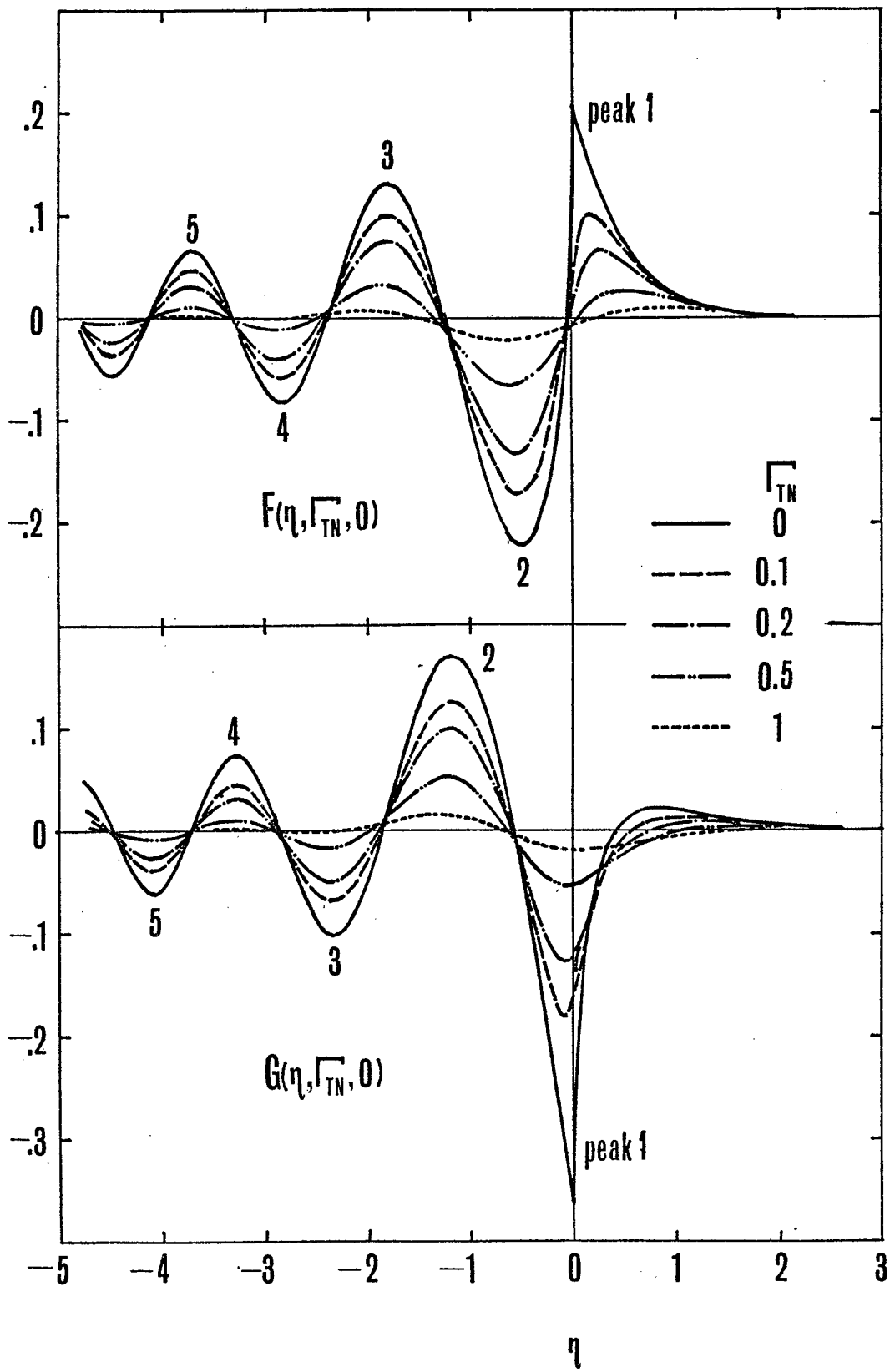

Fig.3.3 Electrooptical functions including thermal broadening effect (a) $F(\eta,\Gamma_{TN},0)$ and (b) $G(\eta,\Gamma_{TN},0)$.[13)]

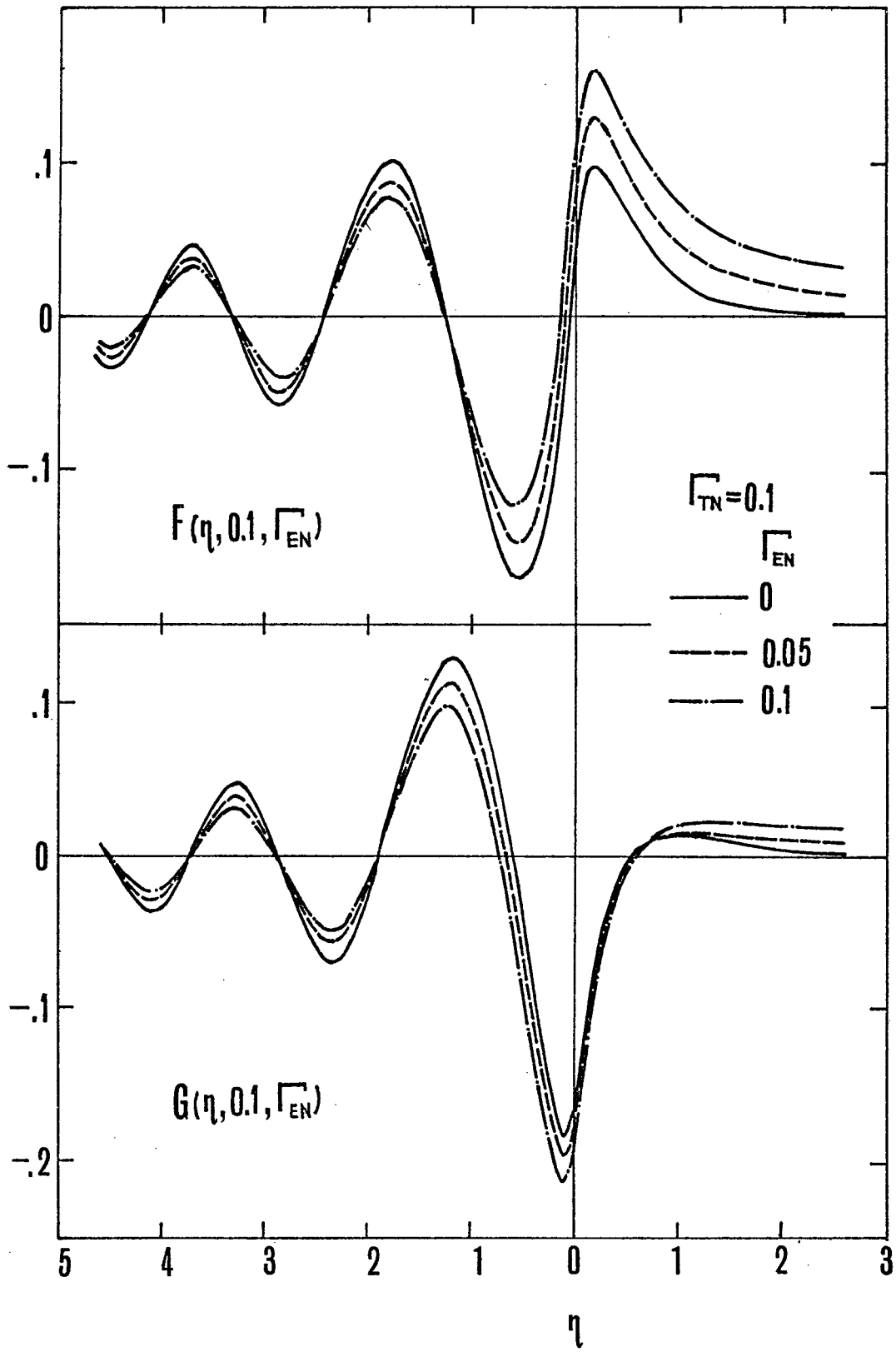

Fig.3.4 Broadened electrooptical functions with both thermal and electric field broadening.[13)]

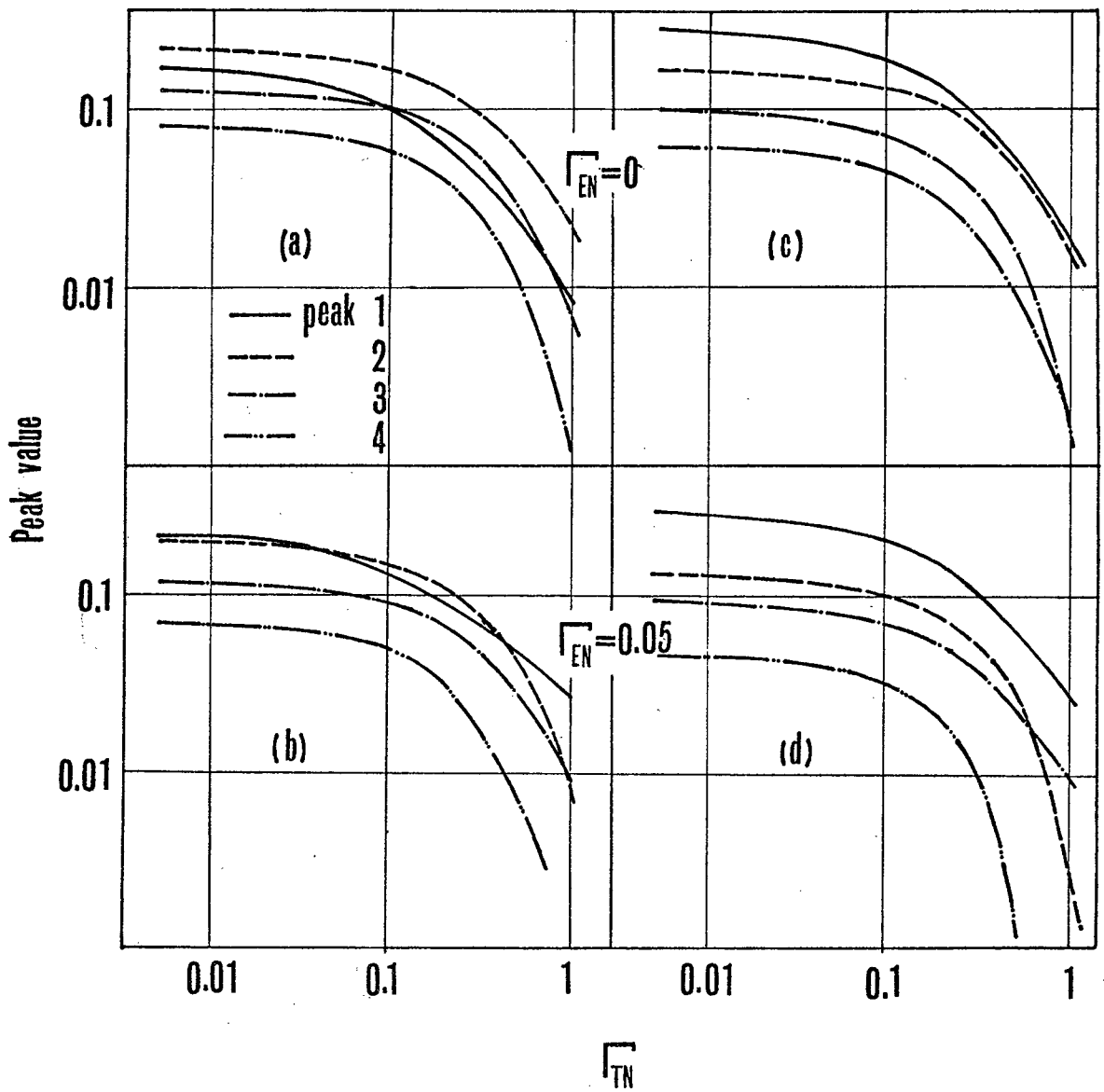

Fig.3.5 The dependence of the peak amplitudes on Γ_{TN} (a) and (c) with only thermal broadening, and (b) and (d) with $\Gamma_{EN}=0.05$.[13] The left hand side corresponds to $F(n,\Gamma_{TN},\Gamma_{EN})$ and right hand side to $G(n,\Gamma_{TN},\Gamma_{EN})$.

of the absolute values of the several peaks of $F(\eta,\Gamma_{TN},\Gamma_{EN})$ and $G(\eta,\Gamma_{TN},\Gamma_{EN})$ upon Γ_{TN} are shown. In the case of only the thermal broadening, they are shown in Fig.3.5(a) and (c). For both $F(\eta,\Gamma_{TN},0)$ and $G(\eta,\Gamma_{TN},0)$, it can be seen that the amplitudes of these peaks do not decrease so much when Γ_{TN} is below 0.1, but the amplitudes are decreasing abruptly with Γ_{TN} beyond a larger Γ_{TN} above 0.1. In the case of both the thermal and electric field broadening, the subsidiary oscillation peaks are decreasing with Γ_{EN} and the decrease of the peak 1 with Γ_{TN} is smaller than without the electric field broadening. These curves correspond to the temperature dependences of the peak values of the signals observed experimentally, and therefore by comparing with experimental data, we can decide the relation between temperature and Γ_{TN}.

3.3.3 Electric Field Dependence

We will examine the dependence of $\Delta\varepsilon_1(\omega,\Gamma_T,\Gamma_E)$ and $\Delta\varepsilon_2(\omega,\Gamma_T,\Gamma_E)$ on electric field. Here we suppose that temperature, therefore, Γ_T, is constant and Γ_E is proportional to electric field. Since θ is proportional to two-third powers of electric field E from Eq.(2.12), and Γ_{TN} and Γ_{EN} are equal to Γ_T/θ and Γ_E/θ, respectively, Γ_{TN} is proportional to $E^{-2/3}$ and Γ_{EN} to $E^{1/3}$. Only the relative behavior of the calculated spectra is treated here in order to utilize them at any critical points for the comparison with both electroabsorption and electroreflectance. In the

electric field dependence of the electrooptical signal, one must take account of the electric field dependence of the coefficient $B\theta^{1/2}/\omega^2$ in Eq.(3.4). Then we introduce an electric field E_0 which is a function of temperature and θ_0 is equal to $(e^2E_0^2/2\mu\hbar)^{1/3}$. Hence the electric field dependence of the coefficient $B\theta^{1/2}/\omega^2$ can be represented by normalized $(E/E_0)^{1/3}$ and the electric field dependent term in $\Delta\varepsilon_1(\omega,\Gamma_T,\Gamma_E)$ or $\Delta\varepsilon_2(\omega,\Gamma_T,\Gamma_E)$ becomes $(E/E_0)^{1/3}$ $F(\eta,\Gamma_{TN},\Gamma_{EN})$ or $(E/E_0)^{1/3}G(\eta,\Gamma_{TN},\Gamma_{TN})$. The electric field dependences of $(E/E_0)^{1/3}F(\eta,\Gamma_{TN},\Gamma_{EN})$ and $(E/E_0)^{1/3}G(\eta,\Gamma_{TN},\Gamma_{EN})$, that is, $\Delta\varepsilon_1(\omega,\Gamma_T,\Gamma_E)$ or $\Delta\varepsilon_2(\omega,\Gamma_T,\Gamma_E)$, are shown in Fig.3.6.(a) and (b). It is assumed now that at $E=E_0$ $\Gamma_{TN}=1.0$ and $\Gamma_{EN}=0.01$. These graphs correspond to the relative change of the electrooptical signal with electric field. For $(E/E_0)^{1/3}F(\eta,\Gamma_{TN},\Gamma_{EN})$, when electric field is relatively small, the peak 1 is almost in the same position in energy for any electric field in spite of the different $\hbar\theta$. When electric field is large, the peak 1 grows much with electric field than the other peaks. For $(E/E_0)^{1/3}$ $G(\eta,\Gamma_{TN},\Gamma_{EN})$, the peak 1 at $\eta=0$ varies little in the position. At the large electric field range the subsidiary oscillation peaks do not so much increase with electric field and tend to saturate. The logarithmic dependence of peak to peak value on electric field is shown in Fig.3.7. In the theory without the broadining, all peaks increase with electric field according to $E^{1/3}$ relation. In the case of only the thermal broadening, they increase abruptly below $E/E_0\simeq10$, and in the

large electric field region the gradients of the logarithmic dependences of the amplitudes on electric field become about 1/2. Forman et al.[12] also calculated this dependence only for the peak 1 and 2 in the electric field range of $E/E_0=0.1\sim40$. This behavior of the thermal broadening can be explained as follows. When electric field is small, Γ_{TN} and its change with electric field are large and so the gradient is abrupt. When electric field is large, Γ_{TN} is very small and so the influence of the broadening to the signal becomes a little and the gradient decreases to be about 1/2. When the electric field broadening is included, the electric field dependence is a little different from the above result. For both $(E/E_0)^{1/3}F(\eta,\Gamma_{TN},\Gamma_{EN})$ and $(E/E_0)^{1/3}G(\eta,\Gamma_{TN},\Gamma_{EN})$, in the case of $\Gamma_{EN}=0.05$ at $E/E_0=1$ the peak to peak values have the linear dependences on the electric field at $E/E_0\simeq1$ and their gradients become gradually small with electric field. The peak to peak values except the one between the peak 1 and peak 2 exhibit a tendency of saturation near $E/E_0\simeq100$. Moreover when Γ_{EN} is larger, they even decrease. These results correspond to the experimental data[8] that in the weak fields the signal grows up abruptly, and in the electric field being still more large it saturates, and finally a little decreases at very large electric fields.

As concerns about the oscillation periods above the energy band edge, the periods are precisely proportional to $E^{2/3}$ in the electrooptical theory without broadening effect. In the calcu-

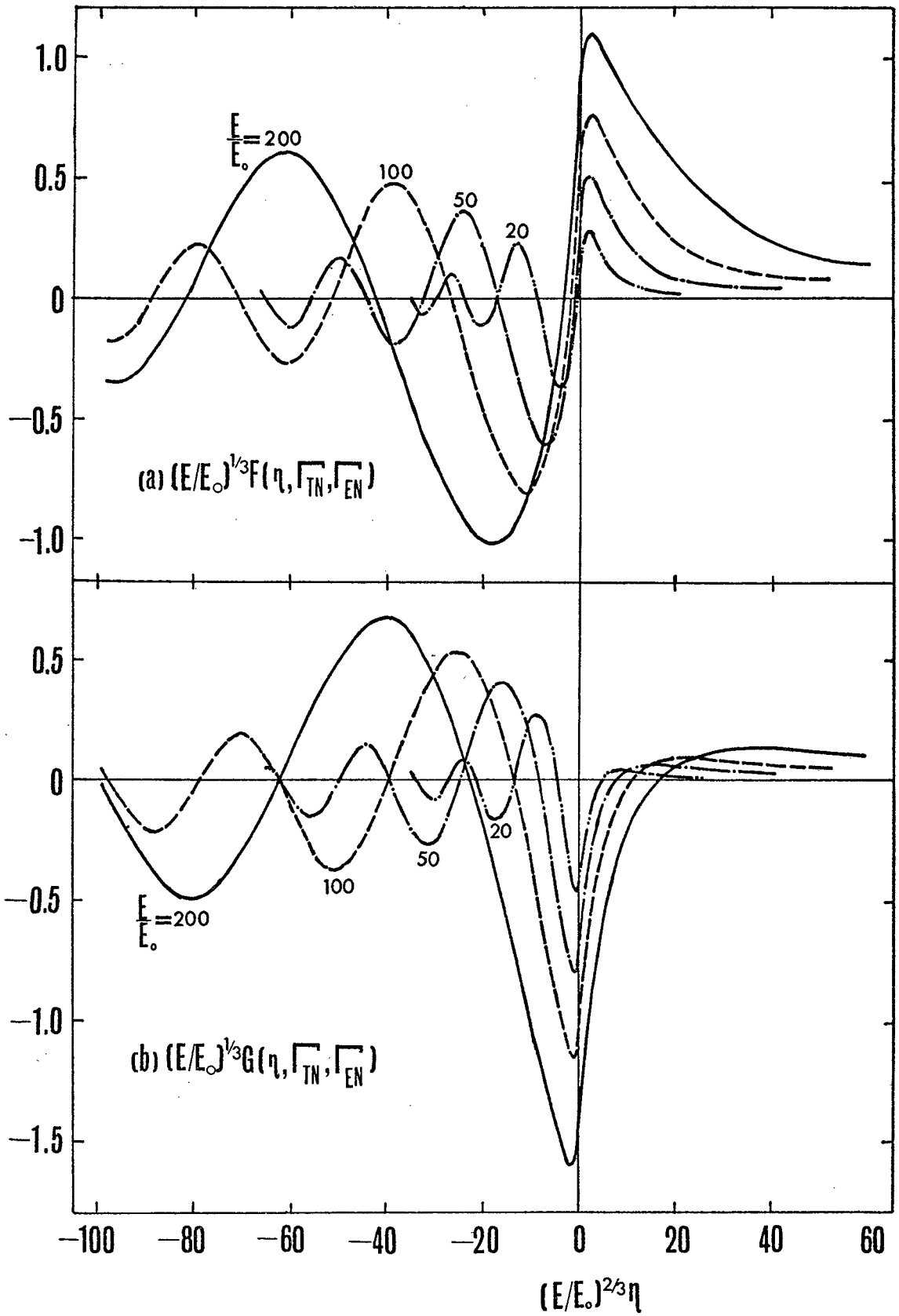

Fig.3.6 The change of the normalized dielectric constant, (a) $(E/E_0)^{1/3} F(\eta, \Gamma_{TN}, \Gamma_{EN})$ and (b) $(E/E_0)^{1/3} G(\eta, \Gamma_{TN}, \Gamma_{EN})$ with electric field.[13)]

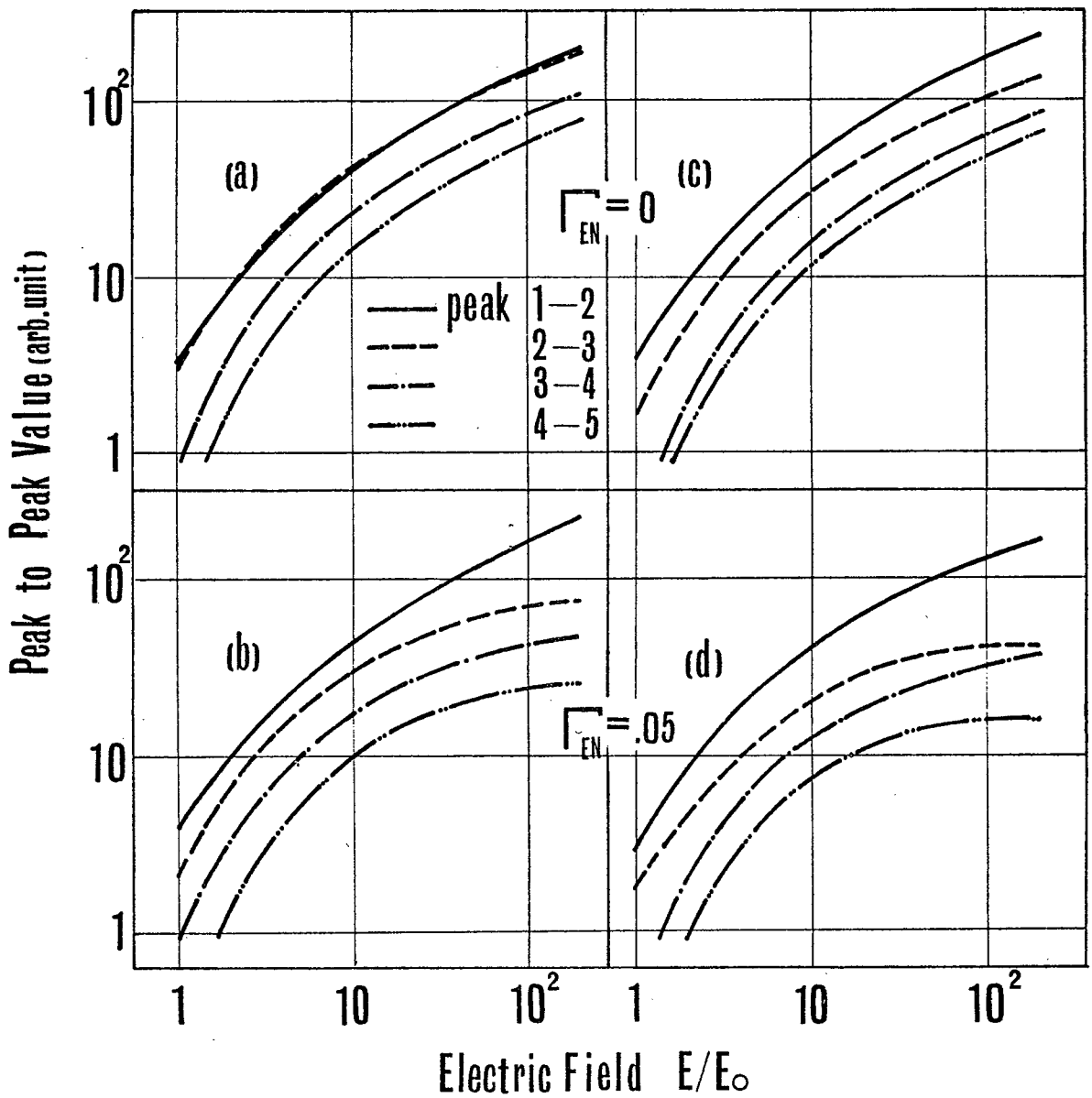

Fig.3.7 The dependence of peak to peak values on electric field E/E_0, at the left hand side for $(E/E_0)^{1/3}F(\eta,\Gamma_{TN},\Gamma_{EN})$ and at the right hand side for $(E/E_0)^{1/3}G(\eta,\Gamma_{TN},\Gamma_{EN})$.[13] (a) and (c) are the curve with only thermal broadening. (b) and (d) are with $\Gamma_{TN}=1.0$ and $\Gamma_{EN}=0.05$ at $E/E_0=1$.

lations of broadened electrooptical functions mentioned above, it has been found that the effects of broadening on the oscillation periods are negligibly small.

3.4 Broadened Electrooptical Functions in One- and Two-dimensional Crystal

3.4.1 Electrooptical Signals in One- and Two-dimensional Crystal

In this section, the broadened electrooptical spectra for 1- and 2-dimensional critical point are calculated with parameters, similarly as Grover et al.,[19] and also their temperature and electric field dependences are investigated. Near one-dimensional M_0 critical point, the field induced change in dielectric constant, $\Delta\varepsilon_1$ and $\Delta\varepsilon_2$, can be obtained similarly as in the 3-dimensional case,

$$\Delta\varepsilon_1 = A_1 \, G_1(\eta) \tag{3.5}$$

and

$$\Delta\varepsilon_2 = A_1 \, F_1(\eta) \ , \tag{3.6}$$

where

$$A_1 = \frac{4\pi e^2 C_{\hbar}^2}{m^2\omega^2\hbar} \left(\frac{2\mu_1}{\hbar\theta}\right)^{1/2} \ ,$$

$$F_1(\eta) = 2\pi Ai^2(\eta) - u(-\eta)\sqrt{-\eta}$$

and

$$G_1(\eta) = 2\pi Ai(\eta)\, Bi(\eta) - u(\eta)\sqrt{\eta} \ .$$

$F_1(\eta)$ and $G_1(\eta)$ functions are plotted with the solid line in Fig. 3.8. In two-dimensional case near M_0 critical point, $\Delta\varepsilon_1$ and $\Delta\varepsilon_2$ can be obtained similarly,

$$\Delta\varepsilon_1 = A_2\, G_2(\eta) \ , \tag{3.7}$$

and

$$\Delta\varepsilon_2 = A_2\, F_2(\eta) \ , \tag{3.8}$$

where

$$A_2 = \frac{2\pi^2 e^2 C_0^2}{m^2\hbar^2\omega^2}\,(\mu_1\mu_2)^{1/2} \ ,$$

$$F_2(\eta) = Ai_1(\kappa\eta) - u(-\eta),$$

$$G_2(\eta) = Gi_1(\kappa\eta) + \frac{1}{\pi}\ln|\kappa\eta| + C,$$

$Ai_1(\eta)$ and $Gi_1(\eta)$ show the integral of $Ai(\eta)$ and $Gi(\eta)$, respectively, $\kappa=2^{2/3}$ and C is constant. $F_2(\eta)$ and $G_2(\eta)$ functions are plotted with the solid line in Fig.3.9. $\Delta\varepsilon_1$ and $\Delta\varepsilon_2$ near the other two-dimensional critical points can be also represented by $F_2(\eta)$ and $G_2(\eta)$. These spectra near critical points have the characteristic structures reflecting the forms of joint density of states, that is the inverse square root and logarithmic divergence, step-like and square root dependence. We examine the effect of lifetime broadening on electrooptical signals. The field induced dielectric constant is calculated in the forms of broadened electrooptical functions. The first and second kind of thermal broadened electrooptical function for n-dimensional (n=1,2) are designated as $F_n(\eta,\Gamma_{TN})$ and $G_n(\eta,\Gamma_{TN})$.

3.4.1 Temperature Dependence

The typical curves of the broadened electrooptical functions, $F_1(\eta,\Gamma_{TN})$ and $G_1(\eta,\Gamma_{TN})$ for 1-dimensional case are shown in Fig.3.8,

and $F_2(\eta,\Gamma_{TN})$ and $G_2(\eta,\Gamma_{TN})$ for 2-dimensional case in Fig.3.9. As shown in these figures, the spikes, the discontinuties and the divergences at critical point are rounded off and the other peaks in the oscillations at $\eta<0$ are gradually damping with the increase of Γ, and this behaviors are similar as in the three-dimensional case. When Γ is proportional to thermal energy kT, these curves show the temperature dependences. For one-dimensional case, the peak 2 of $F_1(\eta,\Gamma_{TN})$ and the peak 1 of $G_1(\eta,\Gamma_{TN})$ are reduced abruptly than the others with the increase of Γ_{TN}, which are caused by the inverse square root dependence of photon energy. For $F_1(\eta,\Gamma_{TN})$ the peak 1 following the band edge tail shifts far from $\eta=0$ and the peak 2 shifts slightly to the negative η side with the increase of Γ_{TN}. On the other hand, for $G_1(\eta,\Gamma_{TN})$ the peak 1 shifts to the positive η side at large Γ_{TN} and the peak 2 shifts to the negative η side at small Γ_{TN}. The other peaks do not almost change the position with Γ. Comparing with three-dimensional case, the peak width of the peak 2 of $F_1(\eta,\Gamma_{TN})$ and the peak 1 of $G_1(\eta,\Gamma_{TN})$ are narrow, and these peaks are very sharp at small Γ_{TN}. For two-dimensional case, in the spectra of $F_2(\eta,\Gamma_{TN})$, the peak 1 following the band edge tail and the peak 2 shift far from the band edge $\eta=0$ with the increase of Γ_{TN}, whereas in the three dimensional case the peak 2 does not change its energy position. The change between the peak 1 and peak 2 is much more abrupt than the others at small value of Γ_{TN}, whereas the change is not so much abrupt in the three-dimensional. These behaviors are attributed

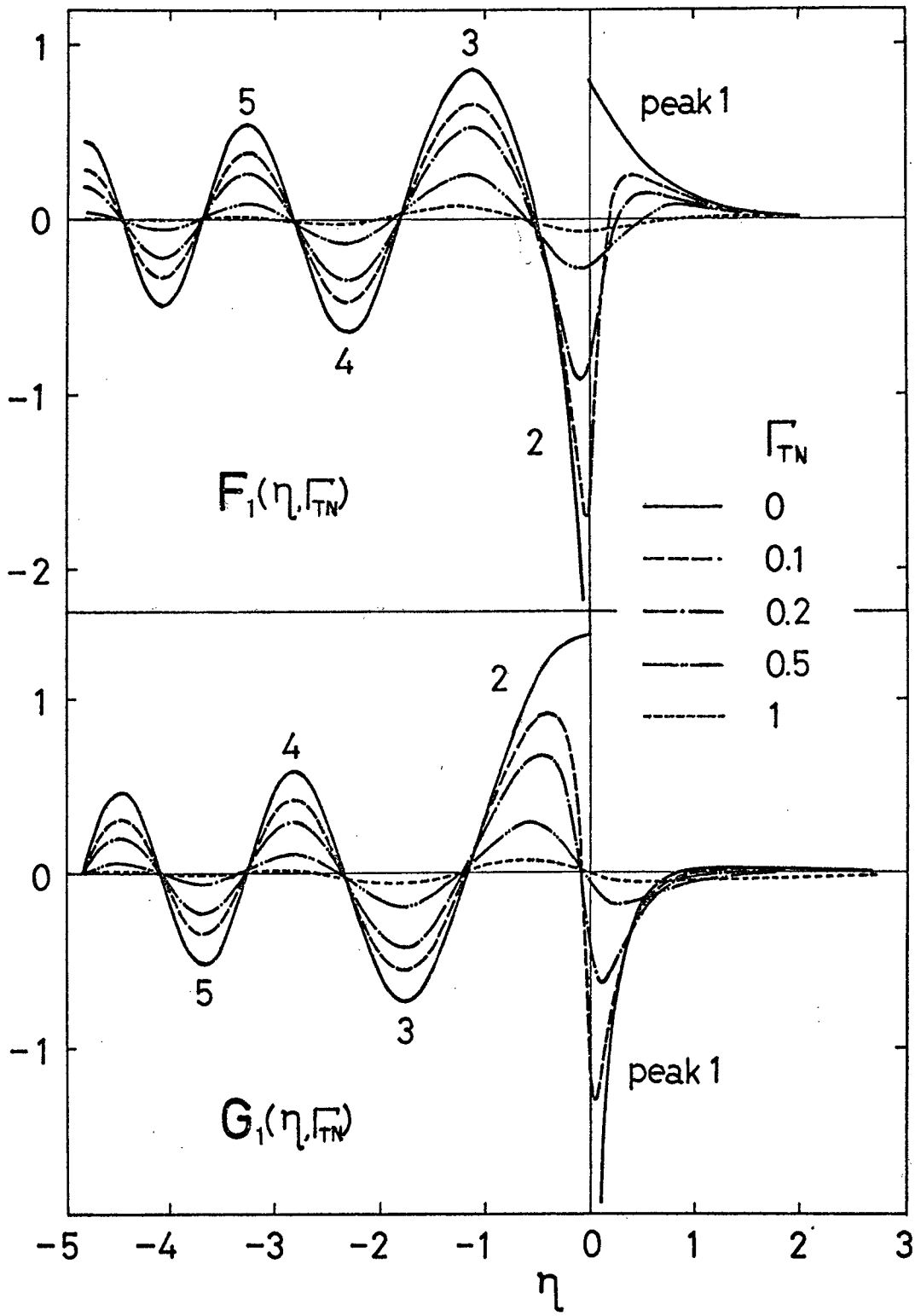

Fig.3.8 Electrooptical functions including thermal broadening effect for 1-dimensional crystal. Solid line is the one without broadening.

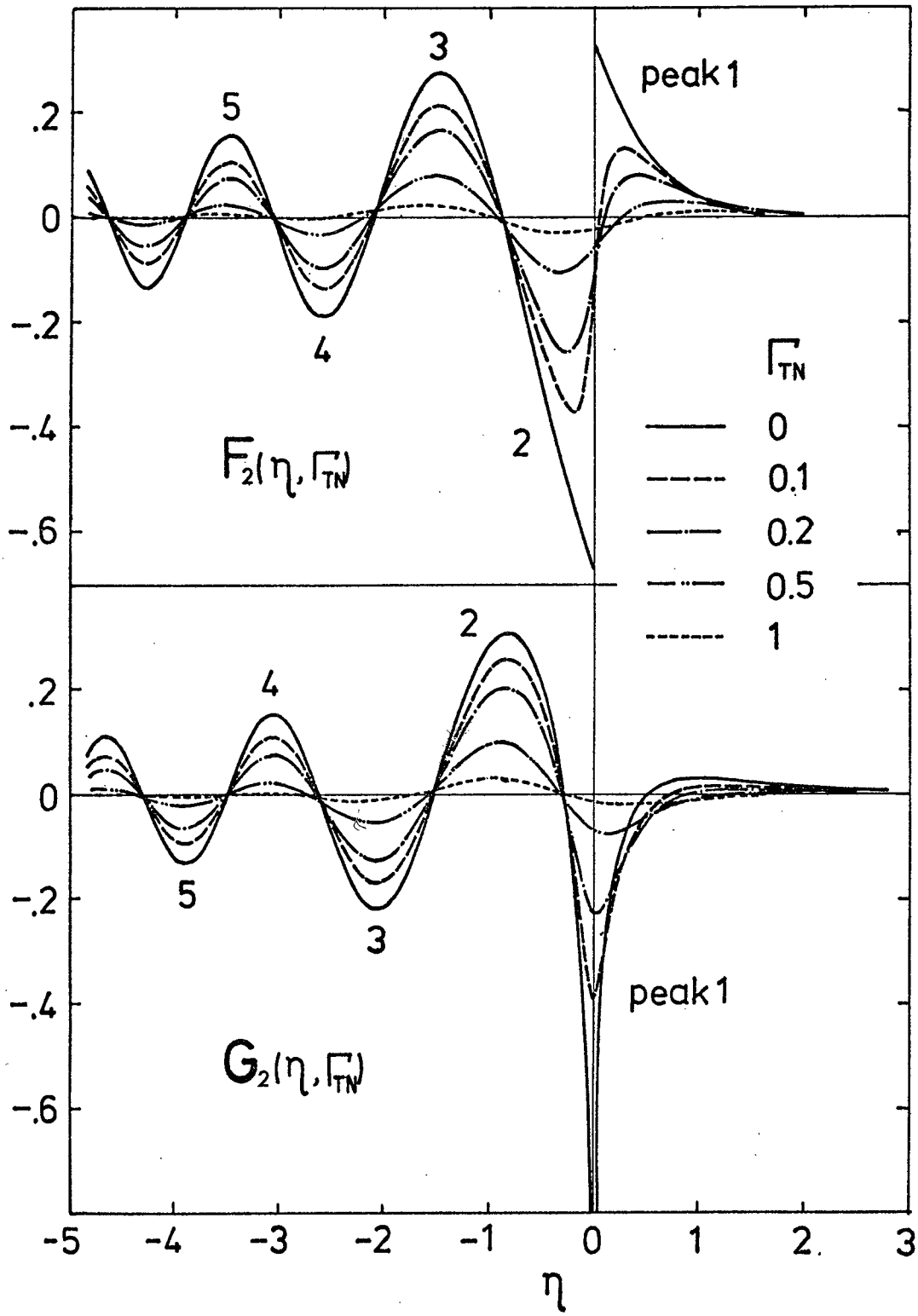

Fig.3.9 Electrooptical functions including thermal broadening effect for 2-dimensional crystal. Solid line is the one without broadening.

to the fact that the joint density of states in the 2-dimensional case is step-function-like at M_0 and M_2 critical point of van Hove singularity and its electrooptical signal has the discontinuty if the broadening effect is not taken into account. As to $G_2(\eta,\Gamma_{TN})$ only peak 1 shifts to the positive η side when Γ_{TN} is fairly large. And also the energy separation of the peak 1 and the peak 2 is smaller than the others for both $F_2(\eta,\Gamma_{TN})$ and $G_2(\eta,\Gamma_{TN})$. The ratio of the energy separations of the peak 1-2 and the peak2-3 is about 0.6 at Γ=0.2 for both $F_2(\eta,\Gamma_{TN})$ and $G_2(\eta,\Gamma_{TN})$, where in the three-dimensional case it is 0.7 for $F(\eta,\Gamma_{TN},0)$ and 1.0 for $G(\eta,\Gamma_{TN},0)$.

3.4.3 Electric Field Dependence

The electric field dependences of $\Delta\varepsilon_1(\omega)$ and $\Delta\varepsilon_2(\omega)$ are examined in this section. Here we assume that temperature is constant, therefore Γ is constant. The normalized broadening factor Γ_{TN} is proportional to $E^{-2/3}$. Only the relative behavior of the calculated spectrum is treated here as well as in the three-dimensional case. An electric field E_0 is introduced in order that Γ_{TN} is equal to 1 at $E=E_0$, and therefore is constant for a certain temperature. And also θ_0 is introduced to be equal to $(e^2E_0^2/2\mu\hbar)^{1/3}$. For one-dimensional case, $(E/E_0)^{-1/3}F_1(\eta,\Gamma_{TN})$ and $(E/E_0)^{-1/3}G_1(\eta,\Gamma_{TN})$ are calculated where $(E/E_0)^{-1/3}$ is the electric field dependent prefactor of electrooptical functions in $\Delta\varepsilon_i(\omega)$, and for two-dimensional case $F_2(\eta,\Gamma_{TN})$ and $G_2(\eta,\Gamma_{TN})$ are calcu-

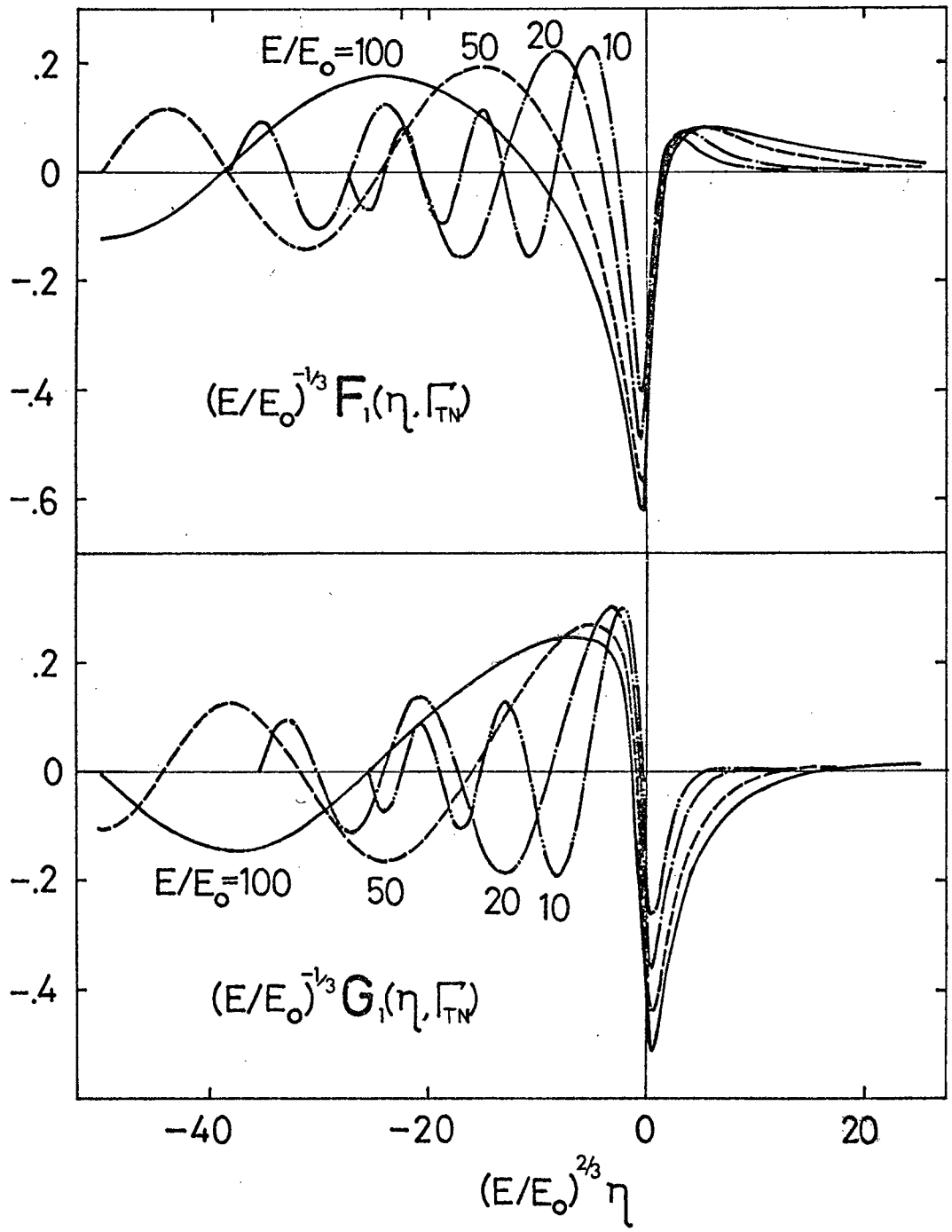

Fig.3.10 The change of normalized dielectric constant for 1-dimensional crystal with electric field. The unit of the abscissa is $(E/E_0)^{2/3}\eta$.

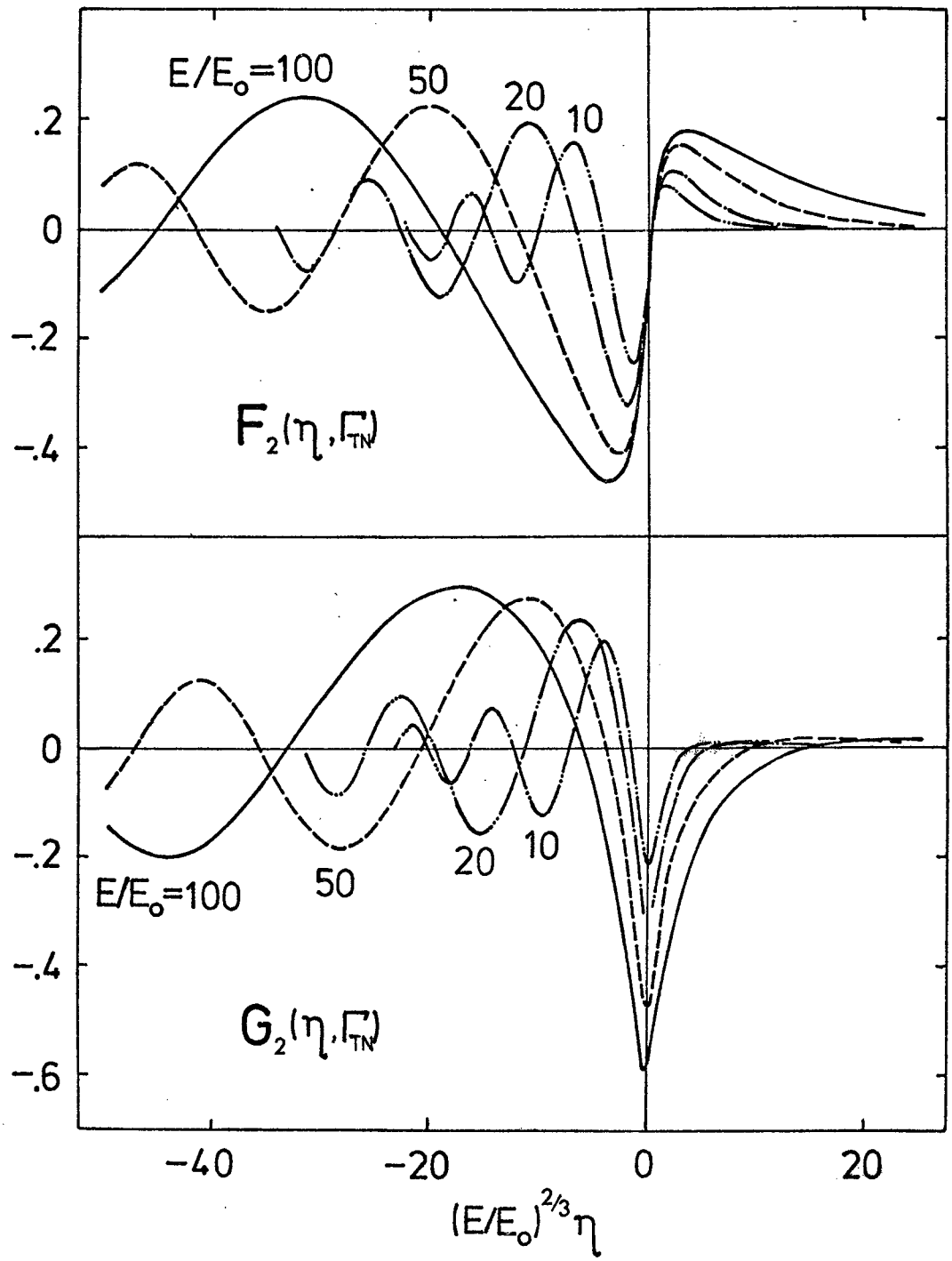

Fig.3.11 The change of normalized dielectric constant for 2-dimensional crystal with electric field. The unit of abscissa is energy $(E/E_0)^{2/3}\eta$.

lated because of the absence of the electric field dependent factor. The electric field dependences of $(E/E_0)^{-1/3}F_1(\eta,\Gamma_{TN})$ and $(E/E_0)^{-1/3}G_1(\eta,\Gamma_{TN})$ corresponding to $\Delta\varepsilon_i(\omega)$ are the shown in Fig.3.10. It can be seen from these curves that at the small field range below $E/E_0 \simeq 10$ all the amplitudes of the signals grow up, and at the large field the peak 2 of $(E/E_0)^{-1/3}F_1(\eta,\Gamma_{TN})$ and $(E/E_0)^{-1/3}G_1(\eta,\Gamma_{TN})$ still grow up because of greater divergence of $\varepsilon(\omega)$ at critical point than the broadening effect, but the other peaks do not grow up or damp because of the field dependent factor $(E/E_0)^{-1/3}$. The electric field dependences of $F_2(\eta,\Gamma_{TN})$ and $G_2(\eta,\Gamma_{TN})$ are shown in Fig.3.11. When electric field becomes large, the amplitudes and oscillation periods of the signals grow up.

3.5 A Comparison with Experiments

In the case that the exciton effect is relatively small, one can directly determine the broadening factors Γ_T and Γ_E from the temperature and electric field dependences of the experimentally observed signals. Even when the exciton effect cannot be neglected, Γ_T and Γ_E can be determined by dealing with the subsidiary peaks which are not so much affected by the exciton effect. Figure 3.12 shows the comparison of the temperature dependences of the third and fourth peaks of the experimental signal with the calculated ones. The experimental data quoted are electroabsorption of germanium worked out by Hamakawa et al.[8] In this method using the electric field modulation in p-n junction, the

effect of the electric field inhomogenity might be considered to be small. The curves in Fig.3.12 represent the peak dependences of $F(\eta,\Gamma_{TN},\Gamma_{EN})$ calculated with Γ_{EN}=0.05. As can be seen in the figure the calculated curve of the fourth peak follows well the experimental plots. Broadening factors can be evaluated from this comparison; Γ_{TN} = 0.45 , 0.13 and 0.020, those are corresponding to 5.0, 1.4 and 0.2 meV, are obtained for 300, 83 and 14 °K respectively. Figure3.13(a) shows a direct comparison of the calculated curve with the experimental signals for 14°K at 10^4V/cm, while the fitting point is chosen at the fourth peak where the contributions of electric field quenching in the exciton absorption might be sufficiently small. A large deviations of the peak 1, 2 and 3 may be attributed to a certain amount of superposition of exciton effect. The calculated curve has the broadening factors of Γ_{TN} = 0.020 and Γ_{EN} = 0.05 whose values are estimated from the temperature dependences of the amplitudes mentioned above. An attempt has been made to plot the difference between the experimental and calculated curves and the result is also shown in Fig.3.13(b). An interesting fact obsereved here is that the line shape of the plot is very similar to that of the exciton electroabsorption, for example, the exciton absorption spectra obtained by Nishino et al. at the same temperature region.[20]

Figure 3.14 shows a comparison between the electroreflectance signal of GaAs[21] and a calculated curve with Γ_{TN}. It is noticed in the analysis that an expected electroreflectance signal

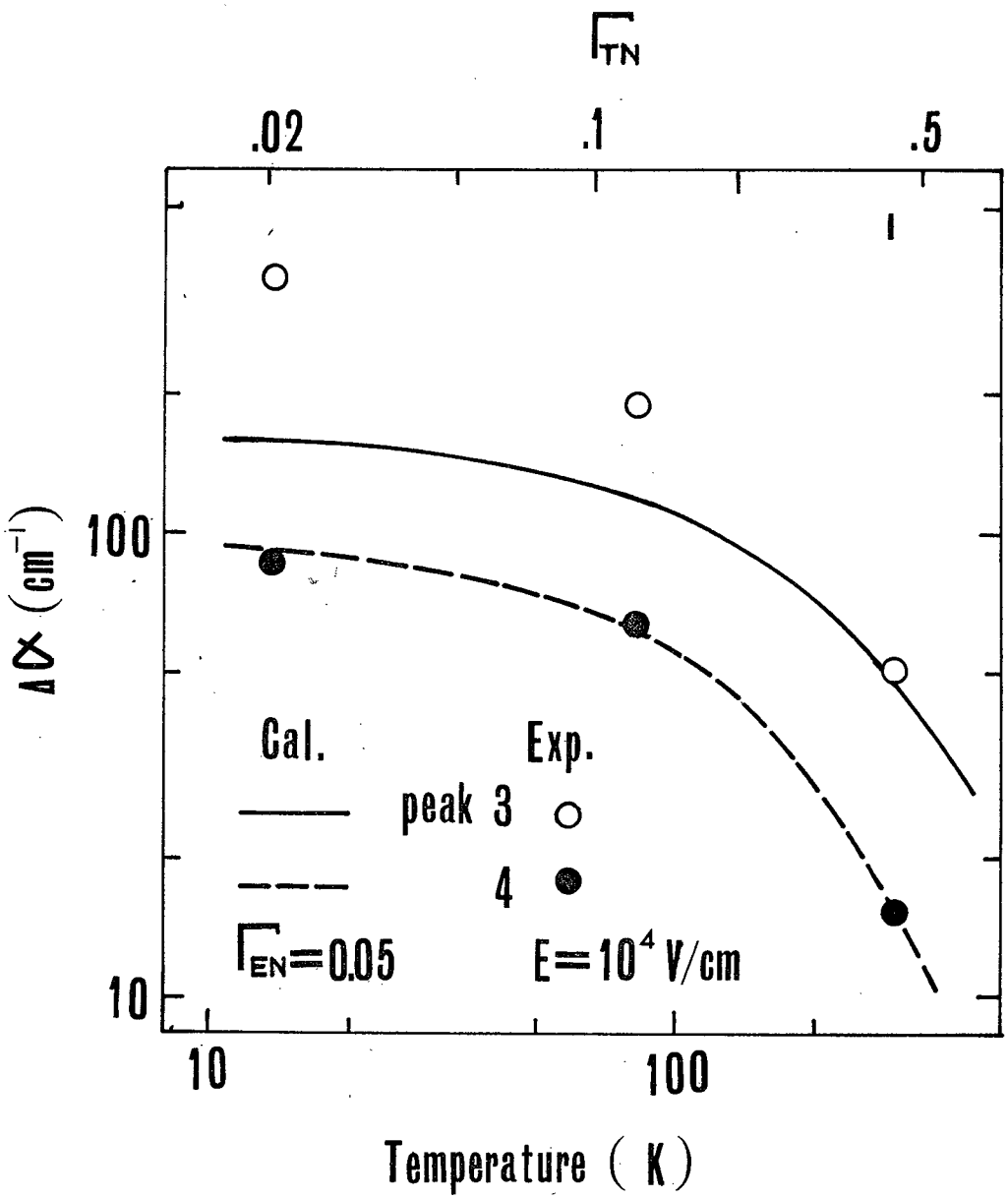

Fig.3.12 The temperature dependences of the third and fourth peak values of the calculated electroabsorption signal. The experimental data of germanium[8] are also plotted.

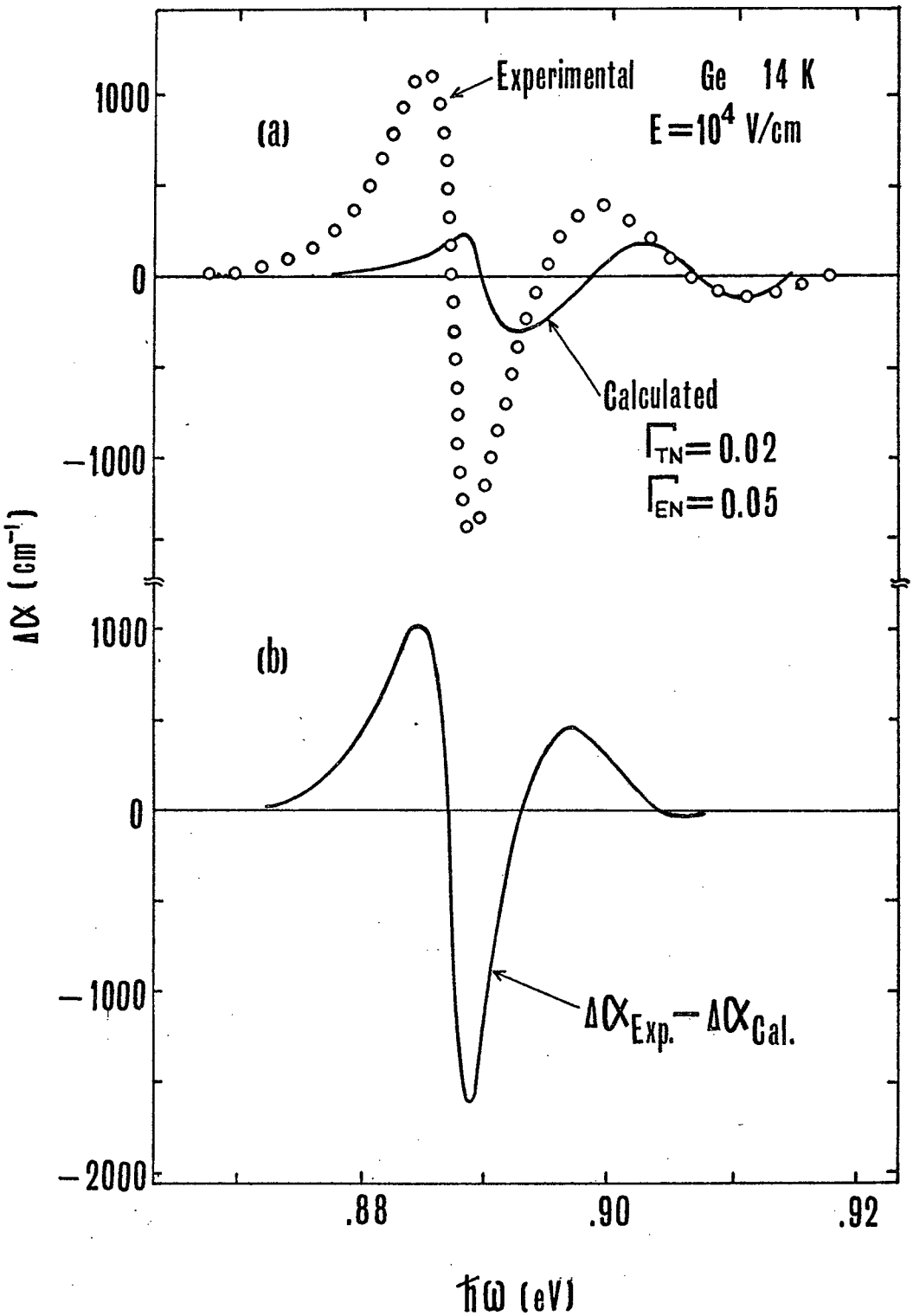

Fig.3.13 A comparison between the experimental signal[8] and the calculated curve with thermal and electric field broadening. (b) The difference between two spectra shown in(a).

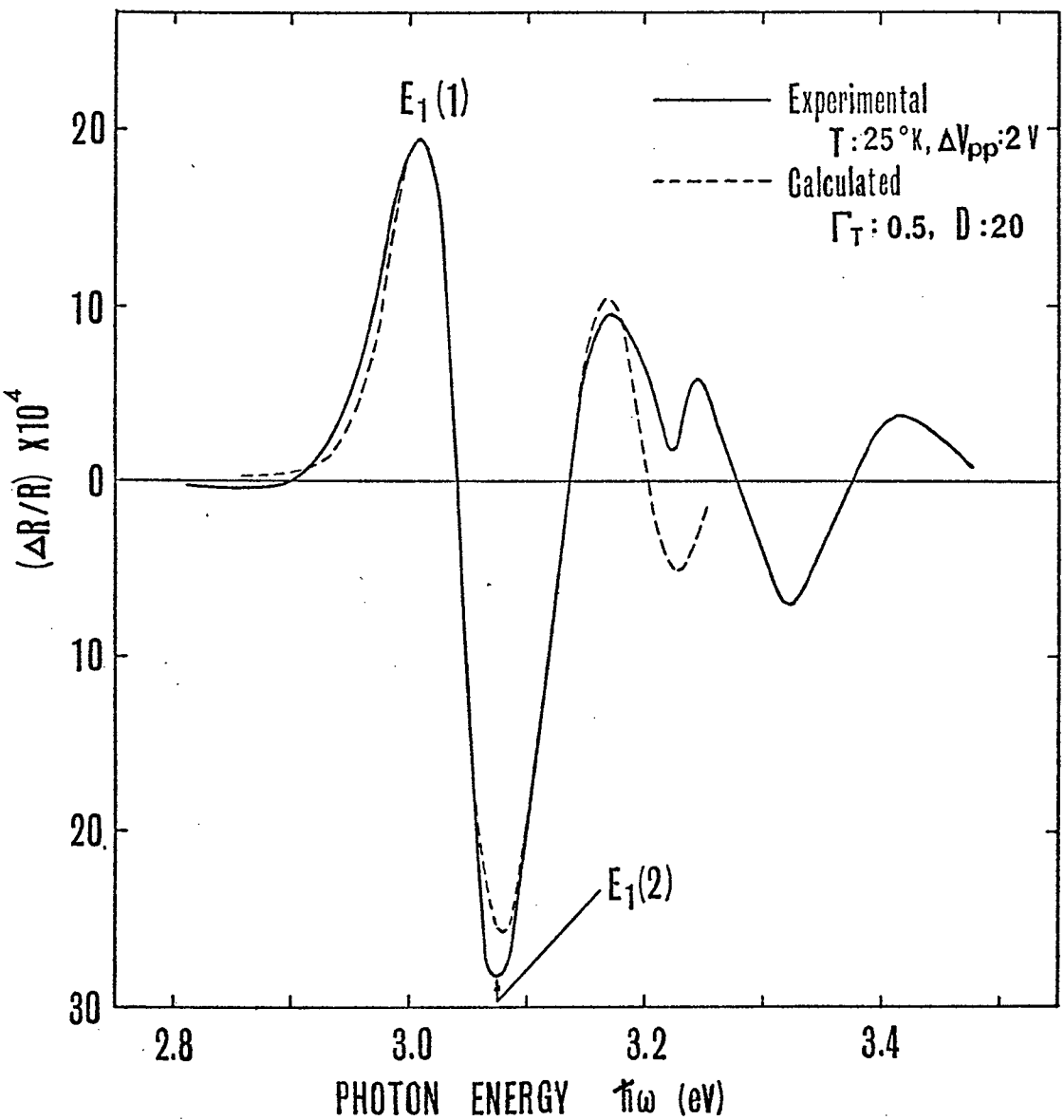

Fig.3.14 A comparison between the electroreflectance signal at 25°K and the calculated spectrum in the case of Γ_{TN}=0.5.(after Nishino, Okuyama and Hamakawa[21])

around 3 eV in GaAs is a nearly equal mixture of $\Delta\varepsilon_1$ and $\Delta\varepsilon_2$, and the mixted signal caused by both contributions of $M_1(\perp)$ and $M_1(//)$ type critical point, is attemped for the different mixture ratio D by considering the anisotropy of the reduced effective mass at Λ critical point. In the figure the calculated spectrum is normalized at the peak position and amplitude of $E_1(1)$, and also the width of the $E_1(2)$ structure are put together to the experimental data. Based upon a good agreement between the calculated and experimental line shape, the electroreflectance spectra were interpreted by the contribution from M_1 critical points including both types of $M_1(\perp)$ and $M_1(//)$, in spite of the discussion of the existence of hyperbolic exciton near this Λ_3-Λ_1 transition edge by Shaklee et al.[22)]

3.6 Summary

In this chapter, the various sources of broadening effect in electrooptical signals have been discussed. The effects of electric field broadening in addition to thermal broadening in the electrooptical function have been calculated. Parametric changes in the amplitudes and oscillation periods with thermal and electric field broadening factors are presented so as to be able to utilize in the quantitative analysis of experimental data. Moreover, the estimations of the broadening factors have been tried from the comparison between the calculated and experimental spectra of Ge and GaAs. The result in Ge shows a considerable

contribution from the exciton electroabsorption at low temperatures.

References

1. C. B. Duke and M. E. Alferieff, Phys. Rev. 145, 583 (1966).
2. H. I. Ralph, J. Phys. C 1, 378 (1968).
3. J. D. Dow and D. Redfield, Phys. Rev. B 1, 3358 (1970), J. D. Dow, B. Y. Lao and S. A. Newman, Phys. Rev. B 3, 2571 (1971).
4. R. Enderlein, Phys. Stat. Sol. 26, 509 (1969).
5. D. F. Blossey, Phys. Rev. B 2, 3976 (1970), D. F. Blossey, *ibid.* 4, 1382 (1971).
6. T. Nishino, Y. Hashimoto, M. Okuyama and Y. Hamakawa, J. Phys. Soc. Japan 26, 1555 (1969).
7. B. O. Seraphin and N. Bottka, Phys. Rev. 145, 628 (1966).
8. Y. Hamakawa, F. A. Germano and P. Handler, Phys. Rev. 167, 703 (1968).
9. D. E. Aspnes, Phys. Rev. 153, 972 (1967).
10. R. Enderlein, Phys. Stat. Sol. 20, 295 (1967).
11. R. Enderlein and R. Keiper, Phys. Stat. Sol. 23, 127 (1967).
12. R. A. Forman, D. E. Aspnes and M. Cardona, J. Phys. Chem. Solids 31, 227 (1970).
13. M. Okuyama, T. Nishino and Y. Hamakawa, Japan. J. Appl. Phys. 7, 1002 (1972).
14. F. Evangelisti and A. Frova, Solid State Commun. 6, 621 (1968).
15. D. E. Aspnes and A. Frova, Solid State Commun. 7, 155 (1969).
16. A. Frova and D. E. Aspnes, Phys. Rev. 182, 795 (1969).
17. S. Koeppen and P. Handler, Phys. Rev. 187, 1182 (1970).

18. D. E. Aspnes and M. Cardona, Phys. Rev. 173, 714 (1968).

19. J. Grover, S. Koeppen an P. Handler, Phys. Rev. B 4, 2830 (1971).

20. T. Nishino, T. Yanagida and Y. Hamakawa, J. Phys. Soc. Japan 30, 579 (1971).

21. T. Nishino, M. Okuyama and Y. Hamakawa, J. Phys. Chem. Solids 30, 2671 (1969).

22. K. L. Shaklee, J. E. Rowe and M. Cardona, Phys. Rev. 174, 828 (1968).

4. ENERGY PARAMETER MODULATION SPECTRA

4.1 Introduction

In recent years, the investigations of optical properties by using the electrooptical effect have been greatly progressed both theoretically and experimentally[1,2]. Among these investigations, the electrooptical effects on the semiconductors have been done not only in three-dimensional crystals but also in chain-like and layer-type crystals.[3] However in progressing the detailed experiment on anisotropic crystal, many difficult problems in the analysis of experimental result open up for the assignment of energy parameters. These difficulties are mainly based upon the broadening effect and their overlapping effect from adjacent edges, which are discussed in the last chapter on three-dimensional crystal, deviations from ideal crystal symmetry etc.

In this chapter the author wishes to expand the theory of broadened dielectric functions of three-dimensional crystals to one- and two-dimensional crystals. In beginning of this calculations a generalized expressions of dielectric functions for 1-, 2- and 3-dimensional crystal is derived. In the calculation of broadened dielectric functions these modulating external perturbations, photon energy $\hbar\omega$, critical point energy $\hbar\omega_g$ and broadening factor Γ, are considered. A systematic relationship has been found in the differential dielectric function modulated with energy parameters of $\hbar\omega$, $\hbar\omega_g$, and Γ. By using the relationship,

one can easily figure the line shape of the modulated spectra for any dimensional critical point from a differential dielectric functions.

4.2 Dielectric Function for 1-, 2- and 3-dimensional Crystal

The complex dielectric function with Lorentzian broadening for direct and allowed interband transition at M_r critical point in n-dimensional crystal may be expressed as the follwing generalized expression,[4]

$$\varepsilon(\omega) = i^{r-n} C_n \int^{\omega-\omega_g+i\Gamma} t^{\frac{n}{2}-2} dt, \qquad (4.1)$$

where

$$C_1 = \frac{\pi e^2 \left|e\cdot P_{if}\right|^2}{m^2\omega^2} \left(\frac{2\mu_1}{\hbar^3}\right)^{1/2},$$

$$C_2 = \frac{2e^2 \left|e\cdot P_{if}\right|^2}{m^2\omega^2} \left(\frac{4\mu_1\mu_2}{\hbar^4}\right)^{1/2},$$

$$C_3 = \frac{e^2 \left|e\cdot P_{if}\right|^2}{m^2\omega^2} \left(\frac{8\mu_1\mu_2\mu_3}{\hbar^5}\right)^{1/2}$$

and other notations are same as in the usual text. Complex dielectric function for each dimension can be easily expressed from this expression. For example, in three-dimensional case it has the square-root singularity near M_r critical point,[5]

$$\varepsilon(\omega) \propto i^{r+1} (\omega-\omega_g+i\Gamma)^{1/2}$$

$$\propto i^r \{-\Phi_3(-x) + i\,\Phi_3(x)\}, \qquad (4.2)$$

where

$$\Phi_3(x) = \left(\frac{x+\sqrt{x^2+1}}{2}\right)^{1/2},$$

$$x = \frac{\omega-\omega_g}{\Gamma}$$

and $i=\sqrt{-1}$. In two-dimensional case it has step-like discontinuity or logarithmic divergence near M_r critical point,

$$\varepsilon(\omega) \propto i^{r+2} \log(\omega-\omega_g+i\Gamma)$$

$$\propto i^r \{\Phi_2^1(x) + i\,\Phi_2^2(x)\}, \qquad (4.3)$$

where

$$\Phi_2^1(x) = \frac{-1}{2\pi} \log(x^2+1),$$

$$\Phi_2^2(x) = \frac{1}{2} + \frac{1}{\pi} \mathrm{Tan}^{-1}x$$

and the logarithmic function is fixed in a Riemann plane. In one-dimensional case it has inverse-square-root divergence near M_r critical point,

$$\varepsilon(\omega) \propto i^{r+1} (\omega-\omega_g+i\Gamma)^{1/2} \qquad (4.4)$$

$$\propto i^r \{\Phi_1(-x) + i\,\Phi_1(x)\},$$

where

$$\Phi_1(x) = \left\{\frac{x+\sqrt{x^2+1}}{2(x^2+1)}\right\}^{1/2}.$$

The energy spectra of these dielectric constants with and without broadening near 1-, 2- and 3-dimensional critical points can be simply illustrated in Fig.4.1. The corresponding line shapes are designated by the number of critical point, r, for each curve

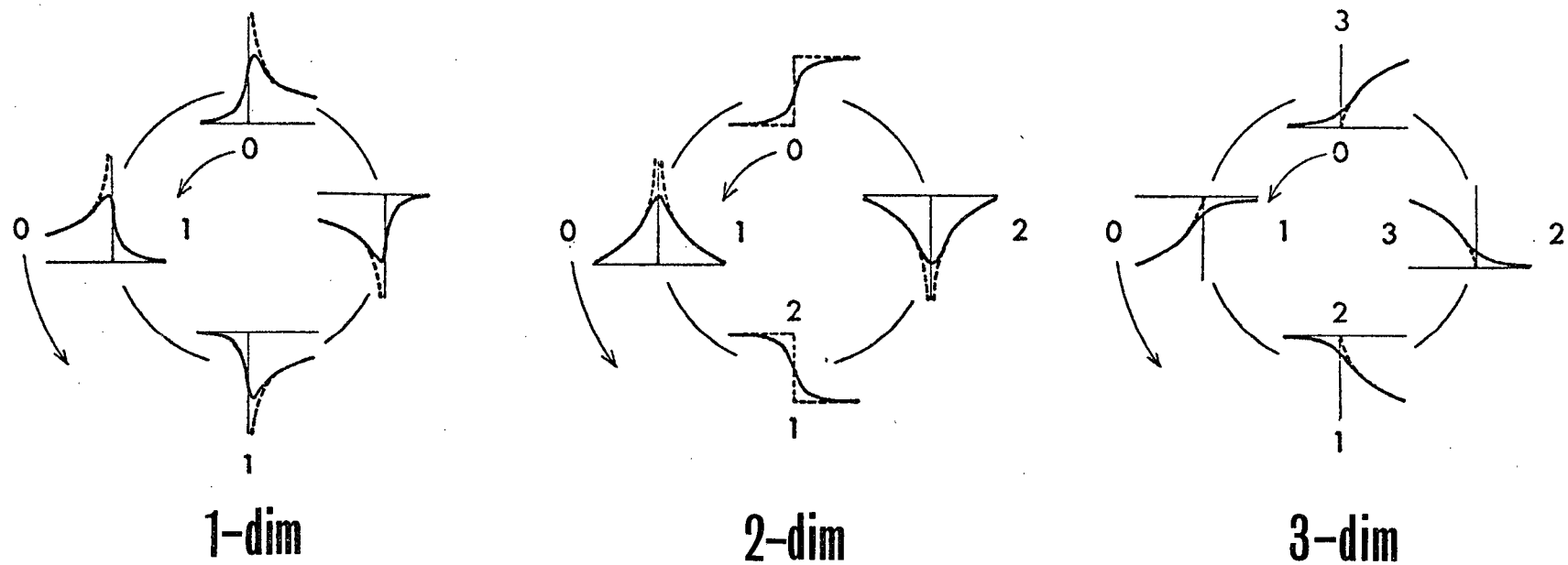

Fig.4.1 A summarized expression of the energy spectra in dielectric constants for one-, two- and three-dimensional crystals; the real(outside) and imaginary(inside) parts of dielectric constant with(solid line) and without(broken line) broadening.[4] The numerals noted in the figure express type of the critical point.

outside the circle to the real part and inside to the imaginary respectively. The real parts shift in phase of 90° from the imaginary.

4.3 Some Relationships between Energy Parameter Modulation Spectra

In modulation spectroscopy, the modulated spectra as wavelength, temperature and stress modulation spectra are expressed by the linear combination of the change in the dielectric constant modulated by some energy parameters. The energy parameter notified here is photon energy $\hbar\omega$ in wavelength modulation, critical point energy $\hbar\omega_g$ and broadening factor Γ in temperature modulation and $\hbar\omega_g$ in stress modulation. These modulation spectra have a close relationship each other since $\varepsilon(\omega)$ can be expressed as the function of $\omega-\omega_g+i\Gamma$,[4]

$$\frac{d\varepsilon(\omega)}{d\omega} = -\frac{d\varepsilon(\omega)}{d\omega_g} = -i\frac{d\varepsilon(\omega)}{d\Gamma} = i^{r-n} C_n (\omega-\omega_g+i\Gamma)^{\frac{n}{2}-2}. \tag{4.5}$$

Separating this to the real and imaginary part,

$$\frac{d\varepsilon_1(\omega)}{d\omega} = -\frac{d\varepsilon_1(\omega)}{d\omega_g} = \frac{d\varepsilon_2(\omega)}{d\Gamma}$$

and

$$\frac{d\varepsilon_2(\omega)}{d\omega} = -\frac{d\varepsilon_2(\omega)}{d\omega_g} = -\frac{d\varepsilon_1(\omega)}{d\Gamma}. \tag{4.6}$$

By using the equation(4.5), one might know the modulated spectra for all energy parameter modulation once one modulation spectrum

is calculated. The physical basis of the relations is that the complex dielectric constant for interband transition can be expressed by the function of the complex energy $\hbar(\omega-\omega_g+i\Gamma)$, where ω^2 included in the prefactor C_n may be neglected because of the small energy dependence to the spectra near critical point. These spectra can be divided into the real and imaginary parts concretely. In three-dimensional case near M_r critical point,[5,6]

$$\frac{d\varepsilon(\omega)}{d\omega} = i^{r+1} C_3\{\phi_3(x) - i\ \phi_3(-x)\}, \tag{4.7}$$

where

$$x = \frac{\omega-\omega_g}{\Gamma}$$

and

$$\phi_3(x) = \frac{1}{\sqrt{\Gamma}} \{\frac{x+\sqrt{x^2+1}}{2(x^2+1)}\}^{1/2}.$$

Peak value of this spectrum is proportional to $\Gamma^{-1/2}$. In two-dimensional case near M_r critical point,

$$\frac{d\varepsilon(\omega)}{d\omega} = i^r\ C_2\ \{-x\phi_2(x) + i\ \phi_2(x)\}, \tag{4.8}$$

where

$$\phi_2(x) = \frac{1}{\Gamma(x^2+1)}.$$

Peak value of this spectrum is proportional to Γ^{-1}. In one-dimensional case near M_r critical point,

$$\frac{d\varepsilon(\omega)}{d\omega} = i^{r+1}\ C_1\ \{\phi_1(x) + i\ \phi_1(-x)\}, \tag{4.9}$$

where

$$\phi_1(x) = \frac{(x+\sqrt{x^2+1})^{1/2}(-2x+\sqrt{x^2+1})}{\sqrt{2\Gamma^3}\ (x^2+1)^{3/2}}.$$

Table 1 A summary of the spectral functions in modulation spectroscopy at various types of edges for one-, two- and three-dimensional crystal.

Dimensions	1		2			3				
Critical point	P_0	P_1	D_0	D_1	D_2	M_0	M_1		M_2	M_3
Sign of μ	+	−	+	+ −	−	+	+	−	+ −	−
ε_1	$\Phi_1(-x)$	$-\Phi_1(x)$	$\Phi_2^1(x)$	$-\Phi_2^2(x)$	$-\Phi_2^1(x)$	$-\Phi_3(-x)$	$-\Phi_3(x)$		$\Phi_3(-x)$	$\Phi_3(x)$
ε_2	$\Phi_1(x)$	$\Phi_1(-x)$	$\Phi_2^2(x)$	$\Phi_2^1(x)$	$-\Phi_2^2(x)$	$\Phi_3(x)$	$-\Phi_3(-x)$		$-\Phi_3(x)$	$\Phi_3(-x)$
$\Delta\varepsilon_1(\omega,E)$	$G_1(-\eta)$	$-G_1(\eta)$	$G_2(-\eta)$	$-F_2(\eta)$ $F_2(-\eta)$	$-G_2(\eta)$	$G_3(-\eta)$	$G_3(\eta)$	$-F_3(-\eta)$	$-G_3(-\eta)$ $F_3(\eta)$	$-G_3(\eta)$
$\Delta\varepsilon_2(\omega,E)$	$F_1(-\eta)$	$F_1(\eta)$	$F_2(-\eta)$	$G_2(\eta)$ $G_2(-\eta)$	$F_2(\eta)$	$F_3(-\eta)$	$-F_3(\eta)$	$G_3(-\eta)$	$-F_3(-\eta)$ $G_3(\eta)$	$F_3(\eta)$
$\frac{d\varepsilon_1}{d\omega}$	$-\phi_1(-x)$	$-\phi_1(x)$	$\phi_2^1(x)$	$-\phi_2^2(x)$	$-\phi_2^1(x)$	$\phi_3(-x)$	$-\phi_3(x)$		$-\phi_3(-x)$	$\phi_3(x)$
$\frac{d\varepsilon_2}{d\omega}$	$\phi_1(x)$	$-\phi_1(-x)$	$\phi_2^2(x)$	$\phi_2^1(x)$	$-\phi_2^2(x)$	$\phi_3(x)$	$\phi_3(-x)$		$-\phi_3(x)$	$-\phi_3(-x)$
$\frac{d\varepsilon_1}{d\omega g}$	$\phi_1(-x)$	$\phi_1(x)$	$-\phi_2^1(x)$	$\phi_2^2(x)$	$\phi_2^1(x)$	$-\phi_3(-x)$	$\phi_3(x)$		$\phi_3(-x)$	$-\phi_3(x)$
$\frac{d\varepsilon_2}{d\omega g}$	$-\phi_1(x)$	$\phi_1(-x)$	$-\phi_2^2(x)$	$-\phi_2^1(x)$	$\phi_2^2(x)$	$-\phi_3(x)$	$-\phi_3(-x)$		$\phi_3(x)$	$\phi_3(-x)$
$\frac{d\varepsilon_1}{d\Gamma}$	$-\phi_1(x)$	$\phi_1(-x)$	$-\phi_2^2(x)$	$-\phi_2^1(x)$	$\phi_2^2(x)$	$-\phi_3(x)$	$-\phi_3(-x)$		$\phi_3(x)$	$\phi_3(-x)$
$\frac{d\varepsilon_2}{d\Gamma}$	$-\phi_1(-x)$	$-\phi_1(x)$	$\phi_2^1(x)$	$-\phi_2^2(x)$	$-\phi_2^1(x)$	$\phi_3(-x)$	$-\phi_3(x)$		$-\phi_3(-x)$	$\phi_3(x)$

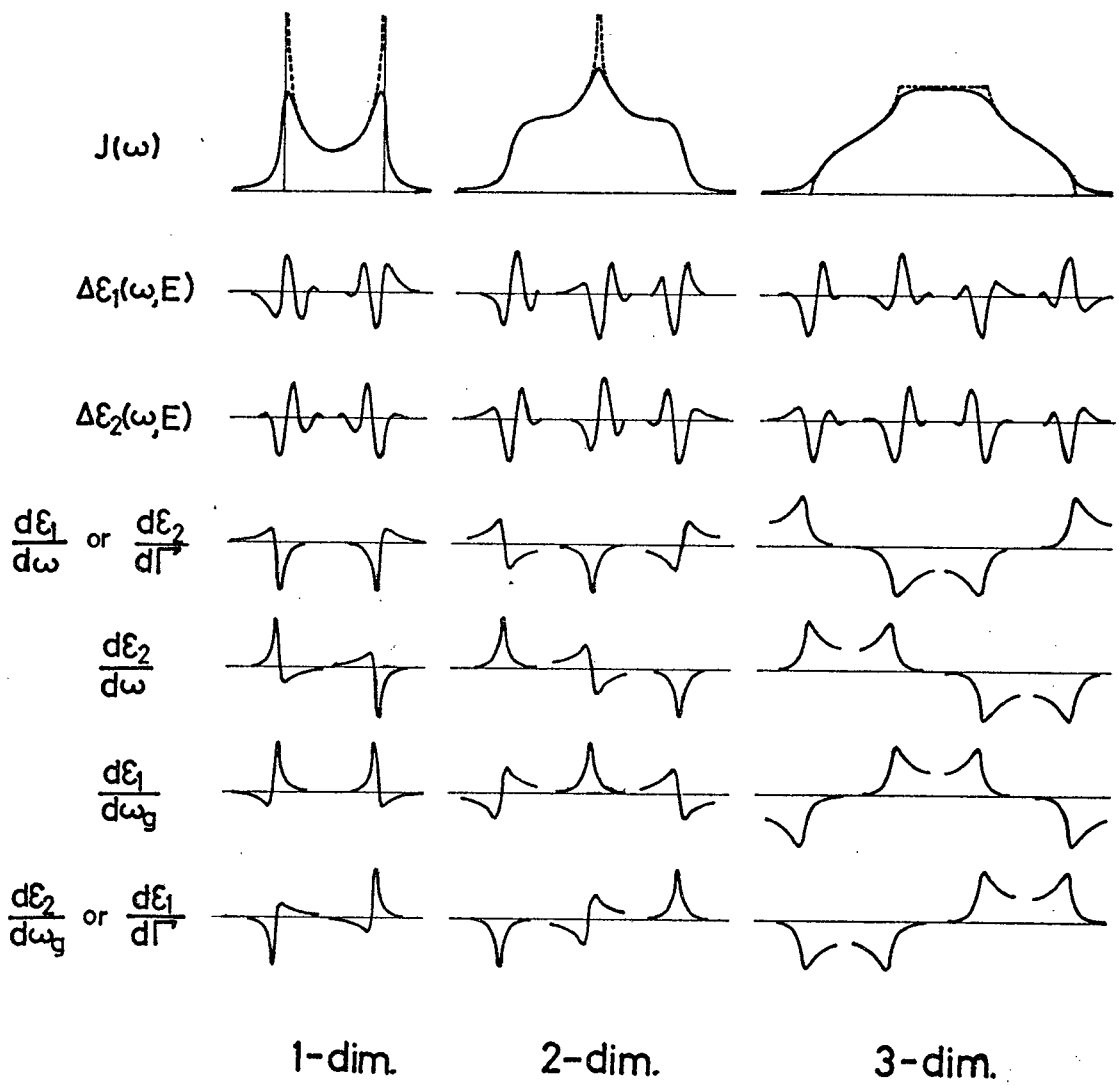

Fig.4.2 A summary of the energy spectra in modulation spectroscopy at one-, two- and three-dimensional critical point.

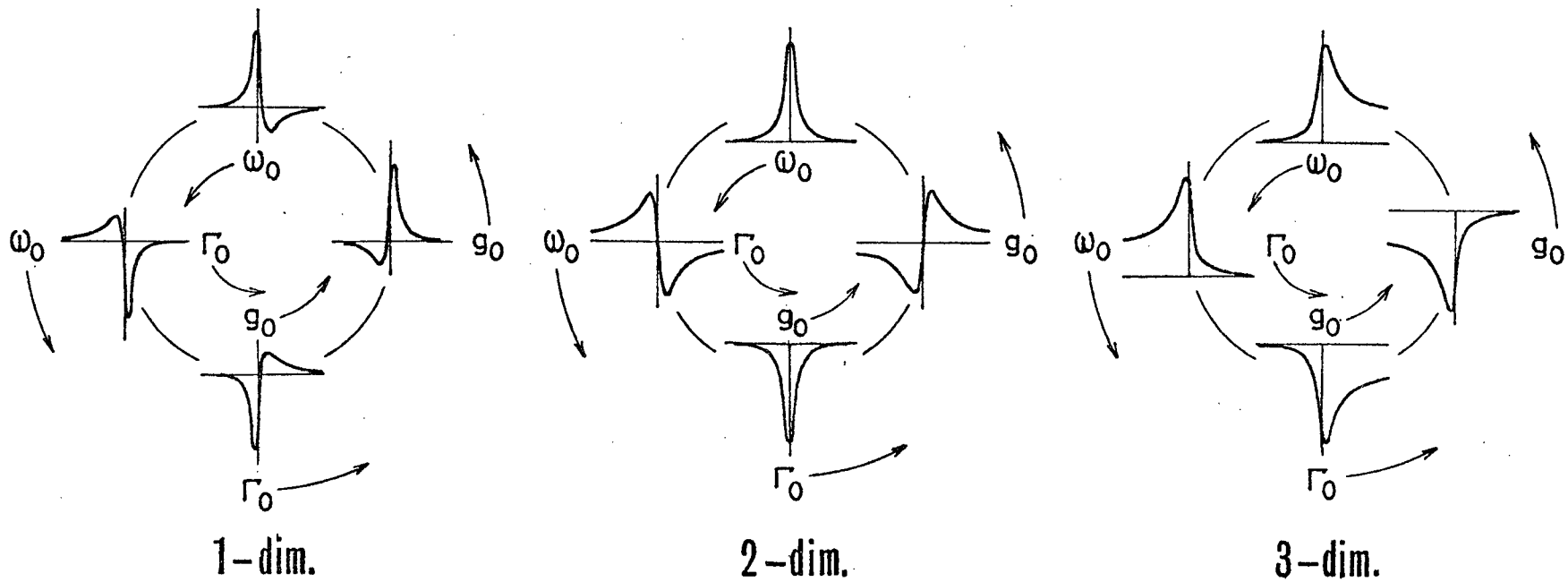

Fig.4.3 A summarized expression of the energy spectra in energy parameter modulation for one-, two- and three-dimensional crystals, the real(outside) and imaginary(inside) parts of the differential dielectric constants modulated by the photon energy $\hbar\omega$, the criticalpoint energy $\hbar\omega_g$ and the broadening factor Γ.[4] The suffix 0 indicates the M_0 critical point, and the arrow means the order of critical point number counterclockwise.

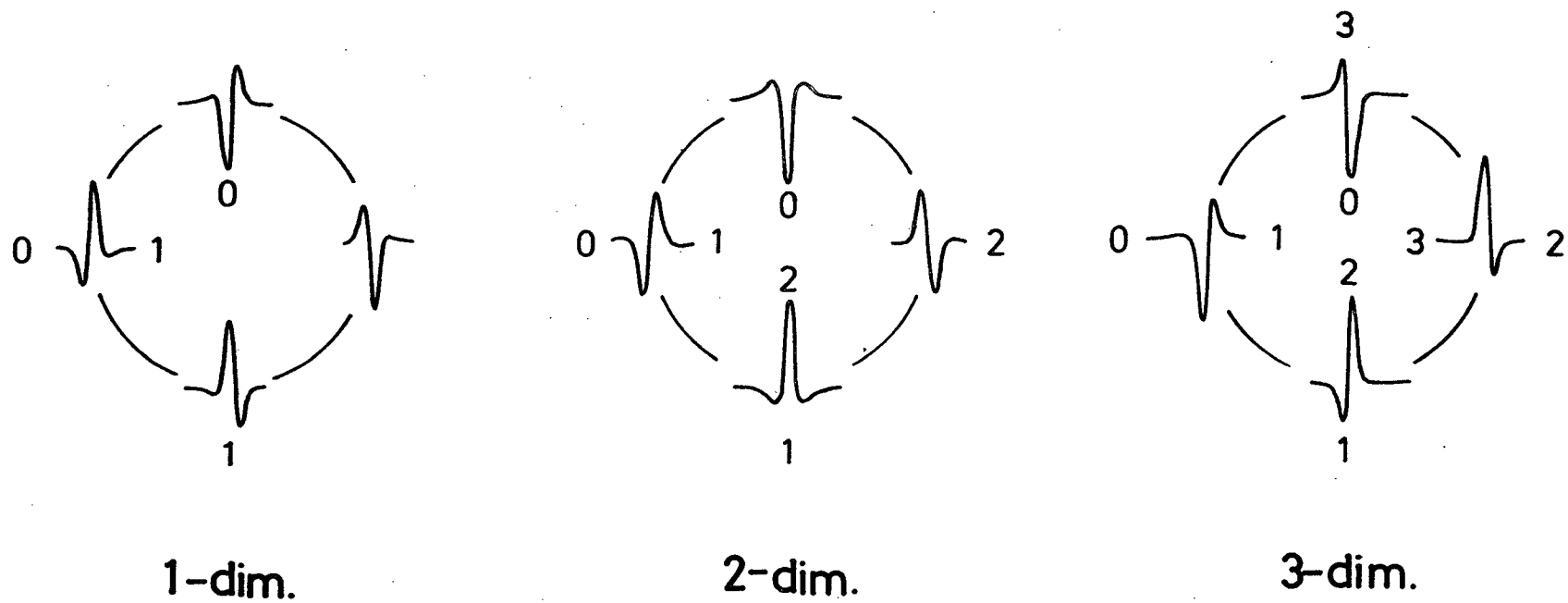

Fig.4.4 A summarized expression of the energy spectra in electrooptical effect with large broadening for one-, two- and three-dimensional crystals. The numerals noted in the figure express type of the critical point for the real(outside) and for the imaginary(inside).

Peak value of this spectrum is proportional to $\Gamma^{-3/2}$. These expressions imply that their configurations are not changed with value of Γ, that is temperature, but the amplitudes of the peaks decrease with Γ and their dependences are different in each dimensional case. From the measurement of temperature dependences of the amplitude in any energy parameter modulated spectra, one might know whether electronic structure tends to be chain-like, layer-type or cubic. All modulated spectra near all dimensional critical point are summarized in Table 4.1, where $\phi_2^{\frac{1}{2}}(x)=-x\phi_2(x)$ and $\phi_2^{\frac{2}{2}}(x)=\phi_2(x)$. Moreover all the spectra are figured in Fig.4.2 in order to call in our minds immediately. Eventually, using these relationships, the real and imaginary parts of these broadened differential spectra of complex dielectric constant are simply expressed in Fig.4.3. The electrooptical spectra with large broadening expressed by the third derivative of the dielectric constant[7] are also summarized in Fig.4.4.

4.4 A Comparison with Experimental Results

A direct comparison between the experimental data and the calculated spectra can be achieved when an exciton effect is relatively small. In Fig.4.5 the spectra of temperature modulation of PbS worked out by Nishino et al.[8] are shown and the best fitted curves of the calculated $\frac{d\varepsilon_2}{d\omega_g}$ are plotted together. PbS is a very relevant material here as its exciton Bohr radius is very large and therefore the effect to the absorption spectra can

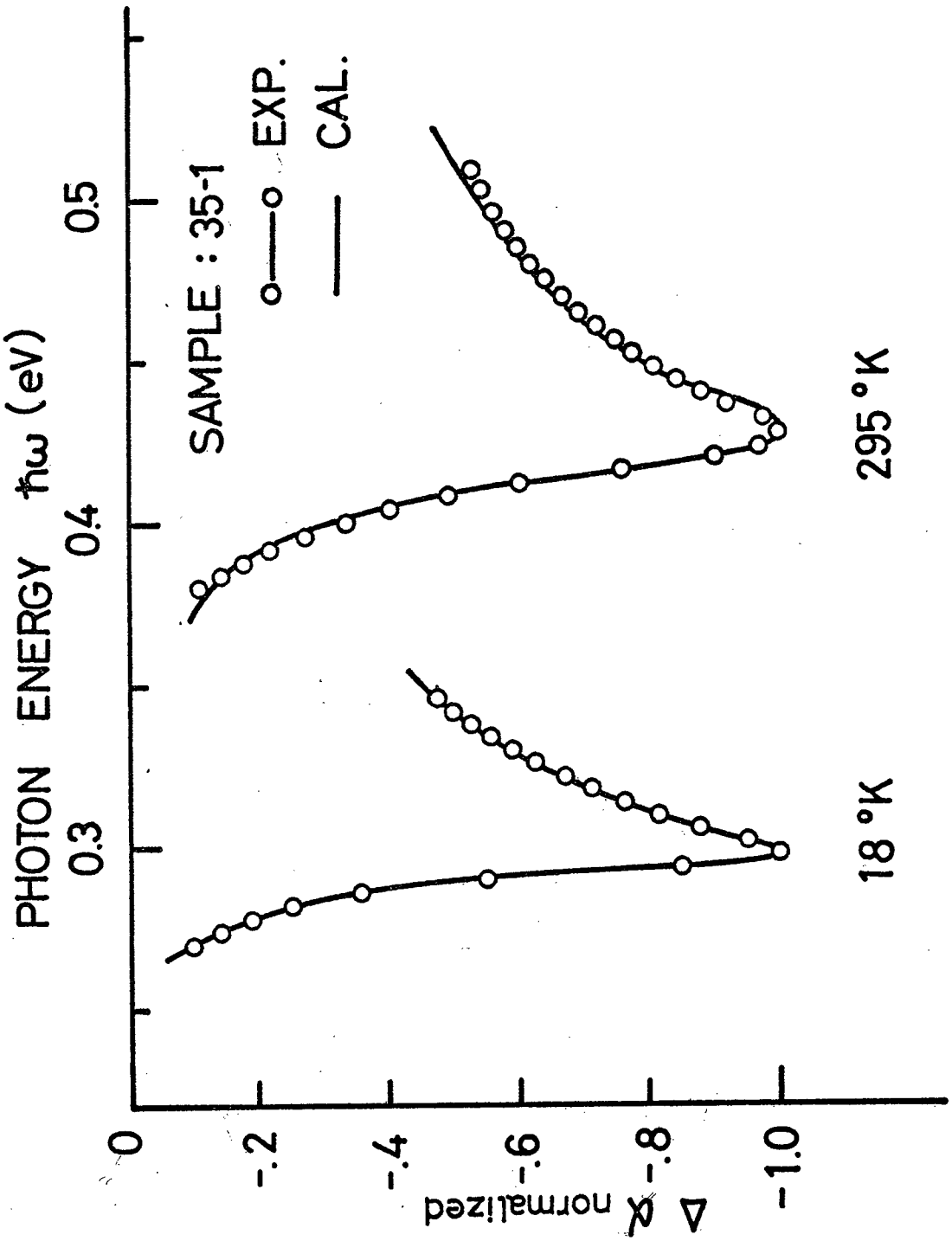

Fig.4.5 An example of the comarison between thermoabsorption spectra of lead sulphide[8] and the calculated curve.

be neglected. The sign of the temperature coefficient $\frac{d\omega_g}{dT}$ of band gap energy in PbS is positive, whereas in ordinary semiconductors it is negative. Hence the measured spectra are directly proportional to the imaginary part of the derivative of dielectric constant drawn in Fig.4.3. The calculated curves agree well with the experimental and it is shown that these spectra of temperature modulation almost consist of only the spectra differentiated by critical point energy. The component of the modulated spectra by Γ is very small as compared with the spectra by ω_g because of $\frac{dE_g}{dT} = 5.5 \times 10^{-4}$ eV/deg. and $\frac{d\Gamma}{dT} = 0.3 \times 10^{-4}$ eV/deg.

4.5 Summary

A generalized expression of broadened complex dielectric functions near one-, two- and three-dimensional critical points has been demonstrated as functions of parameters of photon energy $\hbar\omega$, critical point energy $\hbar\omega_g$ and broadening factor Γ. This expression is resolved to the real and imaginary part of dielectric constant near each critical point and is summarized in Fig.4.1. A systematic relationship has been found in differential dielectric function modulated with energy parameters of ω, ω_g, and Γ and their spectra are easily calculated by the differentiation of the generalized expression. By using the relationship, the line shapes of the modulated spectra for any dimensional critical point can be easily figured from a differential function.in Fig.4.3. A comparison between the theoretical curve and the thermo-

absorption spectra of PbS was tried and shows a good agreement because of the weak effect of exciton.

References

1. M. Cardona, in *Solid State Physics* suppl.11, Ed. by F. Seitz, D. Turnbull and H. Ehrenreich (Academic Press, New York, 1969).
2. B. O. Seraphin et al., in *Semiconductors and Semimetals* 9, Ed. by R. K. Willardson and A. C. Beer (Academic Press, New York, 1972).
3. Y. Suzuki, Y. Hamakawa, H. Kimura, H. Komiya and S. Ibuki, J. Phys. Chem. Solids 31, 2217 (1970)
4. M. Okuyama, T. Nishino and Y. Hamakawa (to be published in J. Phys. Soc. Japan, 1973).
5. E. Matatagui, A. G. Thompson and M. Cardona, Phys. Rev. 176, 950 (1968).
6. B. Batz, Solid State Comm., 5, 985 (1967).
7. D. E. Aspnes and J. E. Rowe, Phys. Rev. B 5, 4022 (1972).
8. T. Nishino, H. Ogawa and Y. Hamakawa, J. Phys. Soc. Japan February (1973).

5. MODULATED SPECTRA IN ANISOTROPIC CRYSTALS

5.1 Introduction

The investigations of optical properties in solids have been made mainly in three-dimensional crystal whose electronic structure is well known. Recently for the anisotropic materials[1] such as chain-like or layer-type crystal the experimental investigations have been accumulated in the optical property but the systematic informations in electronic band structure have not yet been obtained well. One-dimensional motion of electron is realized not only in the chain-like crystal such as $A^{V}B^{VI}C^{VII}$ [2] but also in the solid under strong magnetic field, and is restricted in the direction parallel to the applied magnetic field. For laver-type crystal, the energy band structure and optical properties have been discussed as concern about the two-dimensional crystal by many workers. It is found that for the electroreflectance in the higher interband,[3] the spectra agree with the two-dimensional calculated spectra rather than the three-dimensional. Quite recently it is also reported by Jellito[4] that the density of states in the f. c. c. lattice has a logarithmic divergence at the critical point. As concerns about two-dimensional Wannier exciton the absorption spectra are calculated with and without magnetic field by a few workers.[5-7] But these complete one- or two-dimensional calculation, which was treated in the last section, could not obtain a good agreement with the experimental. Recent-

ly morphology in the optical spectra in the intermediate anisotropic crystals, which include the interaction between layers or chains, was discussed by Nakao[8] and he found the characteristic transition corresponding to the anisotropic parameter. In this section, the modulated spectra with broadening are calculated for these intermediate anisotropic crystals.

5.2 Dielectric Constants with Broadening in Layer-type and Chain-like Anisotropic Crystals

We assume the dependence of energy on wave vector k for orthorhombic crystal structure and nearest-neighbor tight binding approximation as Nakao's work;[8]

$$E(k) = E_c(k) - E_v(k)$$
$$= E_0 - E_1(p\cos k_x + q\cos k_y + r\cos k_z). \quad (5.1)$$

In the case of p=q=r the structure is simple cubic, the case of p=q>>r is layer-type anisotropic and the case of p>>q=r is chain-like anisotropic. Then the joint density of states multiplied by $4\pi^3$ for energy $E=\hbar\omega$ is represented as follows;

$$N(E) = \iiint_{B.Z.} dk\ \delta(E-E(k))$$
$$= \int_{-p}^{p}\int_{-q}^{q}\int_{-r}^{r} dx\,dy\,dz\ \frac{\delta(E+x+y+z)}{[(p^2-x^2)(q^2-y^2)(r^2-z^2)]^{1/2}}, \quad (5.2)$$

where energy E(k) is normalized as $(E(k)-E_0)/E_1$, and $x=p\cos k_x$, $y=q\cos k_y$ and $z=r\cos k_z$. By the substitution of $E \to -E$, $x \to -x$,

$y \to -y$ and $z \to -z$, neither the integrand nor the limits of the integral is modified, so that $N(E)$ is an even function and that its configuration is symmetric. $N(E)$ is represented by using either elliptic integrals or Bessel functions, and the representation of elliptic integrals is selected in our case because of the easy understanding of physical meaning and the easy computation by finite limits of integrals. The behavior of the variation of joint density of states, especially the critical point, among 1-, 2- and 3-dimensional crystal was discussed in detail by Nakao,[8] using Bessel function.

First of all, $N(E)$ is considered for layer-type anisotropic crystals, where $p=q=1$ and $0<r<1$. Then $N(E)$ has the finite value in the range of E from $-2-r$ to $2+r$. The integral in Eq.(5.2) can be carried out in some separate energy regions having the boundary at critical point energy. Equation (5.2) is calculated as follows, for $|E|>2+r$

$$N(E) = 0,$$

for $2-r<|E|<2+r$

$$N(E) = \int_{-1}^{1+r-E} dx\, I_1(x), \tag{5.3}$$

for $r<|E|<2-r$

$$N(E) = \int_{-1}^{1-r-E} dx\, I_2(x) + \int_{1-r-E}^{1+r-E} dx\, I_1(x) \tag{5.4}$$

and for $|E|<r$

$$N(E) = \int_{-1}^{r-E-1} dx\, I_1(x) + \int_{r-E-1}^{-r-E+1} dx\, I_2(x) + \int_{-r-E+1}^{1} dx\, I_1(x), \qquad (5.5)$$

where

$$I_1(x) = \frac{1}{\{r(1-x^2)\}^{1/2}} K\left(\sqrt{\frac{(1+r)^2-(E+x)^2}{4r}}\right),$$

$$I_2(x) = \frac{1}{[(1-x^2)\{(1+r)^2-(E+x)^2\}]^{1/2}} K\left(\sqrt{\frac{4r}{(1+r)^2-(E+x)^2}}\right)$$

and $K(x)$ is the first complete elliptic integral.[9] These density of states functions with some anisotropic parameters, are shown in Fig 5.1. The inflections of $N(E)$ in the figure correspond to each critical point. The critical points at $E=-2-r$ and $2+r$ are minimum and maximum point, that are M_0 and M_3 point, and those at $E=-2+r$ and $2-r$ are saddle point. The critical point at $E=-r$ and r are also saddle point and doubly degenerate.

On the other hand, in the chain-like anisotropic crystal, that is $p=1$ and $0<q-r<1$, $N(E)$ has non-zero value in the range of E from $-1-2r$ to $1+2r$. The integral in Eq.(5.2) can be carried out in some cases of energy region having the limit at critical point energy. Then Eq.(5.2) is calculated as follows,

for $|E|>1+2r$,

$$N(E) = 0$$

and for $1<|E|<1+2r$

$$N(E) = \int_{-r}^{r-E+1} dx\ I_3(x), \tag{5.6}$$

where

$$I_3(x) = \frac{1}{\{r(r^2-x^2)\}^{1/2}} K\left(\sqrt{\frac{(1+r)^2-(E+x)^2}{4r}}\right).$$

For the lower energy than 1, the integration is devided into two cases according to the value of anisotropic parameter. This division results from the fact that two saddle point pass each other in energy with anisotropic parameter, r. In the case of $r<0.5$, for $1-2r<|E|<1$

$$N(E) = \int_{-r}^{-r-E+1} dx\ I_4(x) + \int_{-r-E+1}^{r} dx\ I_3(x) \tag{5.7}$$

and for $|E|<1-2r$

$$N(E) = \int_{-r}^{r} dx\ I_4(x), \tag{5.8}$$

where

$$I_4(x) = \frac{1}{[(r^2-x^2)\{(1+r)^2-(E+x)^2\}]^{1/2}} K\left(\sqrt{\frac{4r}{(1+r)^2-(E+x)^2}}\right).$$

In the case of $r>0.5$, for $2r-1<|E|<1$

$$N(E) = \int_{-r}^{-r-E+1} dx\, I_4(x) + \int_{-r-E+1}^{r} dx\, I_3(x) \qquad (5.9)$$

and for $|E|<2r-1$

$$N(E) = \int_{-r}^{r-E-1} dx\, I_3(x) + \int_{r-E-1}^{-r-E+1} dx\, I_4(x)$$

$$+ \int_{-r-E+1}^{r} dx\, I_3(x)\cdot \qquad (5.10)$$

These density of states functions with some anisotropic parameter are shown in Fig.5.2. The inflections of N(E) in Fig.5.2 correspond to the critical points at E=-1-2r,-1+2r, -r, r, 1-2r and 1+2r. The critical points at E=-1-2r and 1+2r are minimum and maximum point, that are M_0 and M_3 critical point. The ones at E=-1+2r and 1-2r are saddle points, and are separated from degenerate saddle point at E=-1 and 1 and incorporated to the minimum and maximum point at E=1 and -1 with increasing r. The critical point at E=-1 and 1 are saddle point and doubly degenerate. These spectra are reduced to the complete 1-, 2- and 3- dimensional case when r=0 or 1.

In three-dimensional case,[4] for $|E|>3$

$$N(E) = 0,$$

for $1<|E|<3$

$$N(E) = \int_{-1}^{2-E} dx\ I(x) \tag{5.11}$$

and for $|E|<1$

$$N(E) = \int_{-1}^{1} dx\ I(x), \tag{5.12}$$

where

$$I(x) = \frac{1}{(1-x^2)^{\frac{1}{2}}}\ K'\left(\frac{|x+E|}{2}\right)$$

and $K'(x)$ is the first complete elliptic integral of the complementary modul.

In 2-dimensional case for $|E|>2$

$$N(E) = 0,$$

and for $|E|<2$

$$N(E) = \pi\ K'\left(\frac{|E|}{2}\right). \tag{5.13}$$

In one-dimensional case for $|E|>1$

$$N(E) = 0$$

and for $|E|<1$

$$N(E) = \frac{\pi^2}{\sqrt{1-E^2}}. \tag{5.14}$$

These 1-, 2- and 3-dimensional spectra are shown in Fig. 5.1 and 5.2 together with the intermediate anisotropic spectra.

The imaginary part of complex dielectric constant for direct interband transition is proportional to the joint density of states. Generally the complex dielectric constant is affected by the finite lifetime of electron on crystalline level and the spectral behavior is modified and smoothed out. This lifetime broadening effect can be represented as the convolution integral of density of states with Lorentzian as in Eq.(3.3) and Lorentzian factor is assumed to be constant over all the photon energy for simplicity. This assumption may be oversimplified, but is very useful to give the outline of the imaginary part of complex dielectric constant.

The optical constants are calculated using the following substitution the δ-function by a normalized Lorentzian peak,

$$\delta(E-\hbar\omega) \rightarrow \frac{1}{\pi} \frac{\Gamma^2}{(\hbar\omega-E)^2+\Gamma^2}.$$

The contribution of the density of states to the imaginary part of complex dielectric constant is thus given by

$$\varepsilon_2(\omega) = A \frac{1}{\pi} \int_0^\infty \frac{\Gamma\, N(E)}{(\hbar\omega-E)^2+\Gamma^2}\, dE \,, \qquad (5.15)$$

where A is the constant containig the momentum matrix element. The real part of complex dielectric constant, $\varepsilon_1(\omega)$, results from Kramers-Kronig transformation of this equation. In fact, for a narrow Lorentzian line $\varepsilon_1(\omega)$ is obtained by replacing the Lorentzian

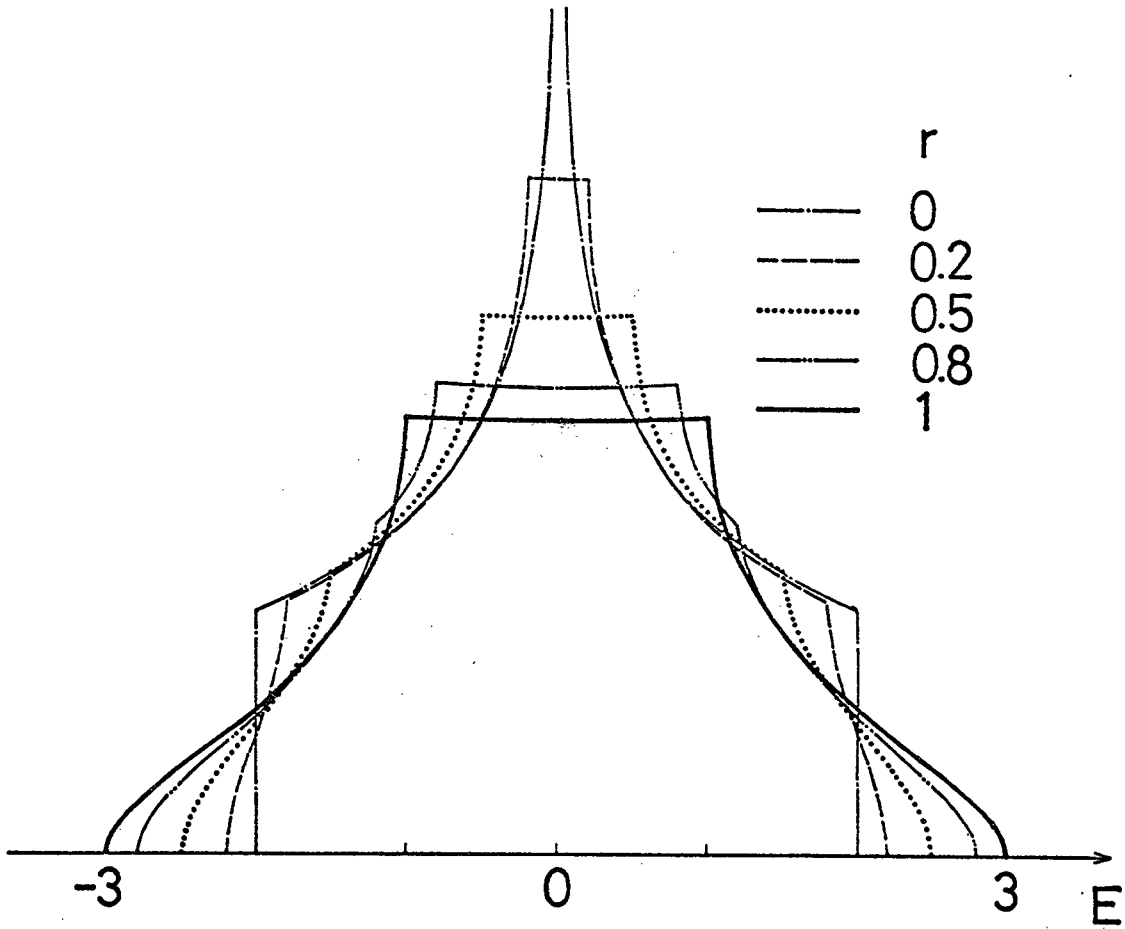

Fig.5.1 The densities of ststes for layer-type electronic structures with some anisotropic parameters.

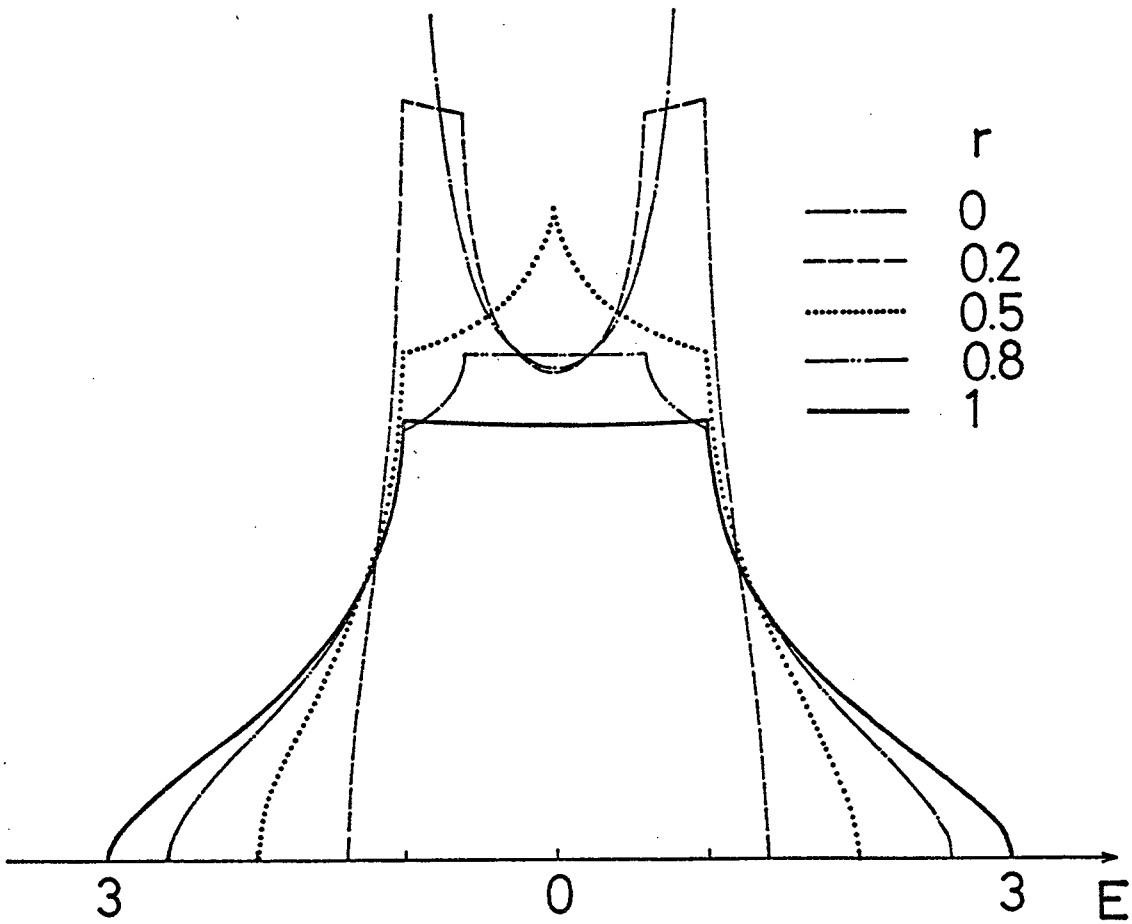

Fig.5.2 The densities of states for chain-like electronic structures with some anisotropic parameters.

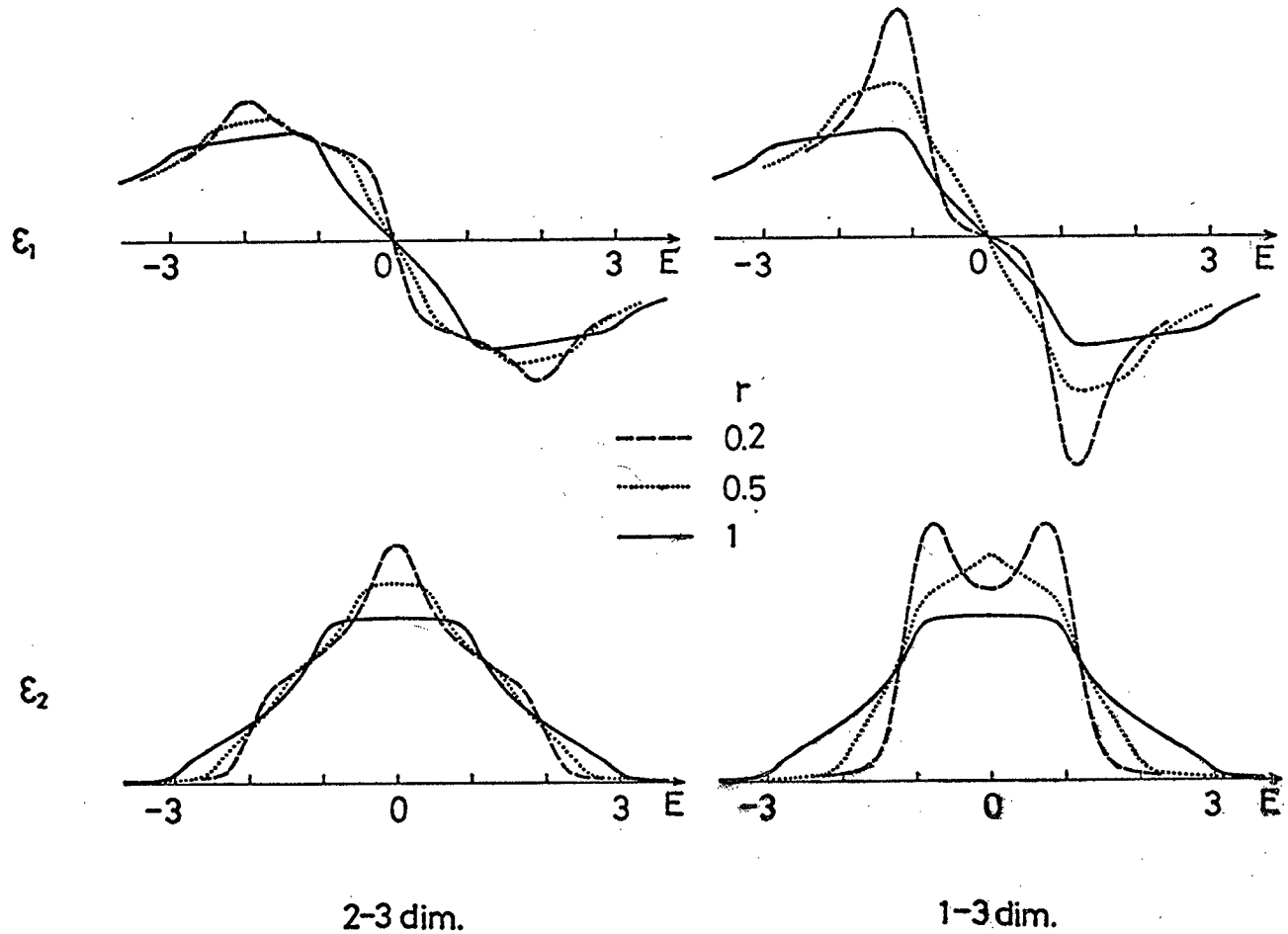

Fig.5.3 The real and imaginary parts of broadened dielectric constants for layer-type and chain-like electronic structure with some anisotropic parameters.

peak by the dispersive Lorentzian line. The broadened real part is given by

$$\varepsilon_1(\omega) = A \frac{1}{\pi} \int_0^\infty \frac{(E-\hbar\omega)N(E)}{(\hbar\omega-E)^2+\Gamma^2} dE. \qquad (5.16)$$

The real and imaginary part of complex dielectric constant are plotted with some anisotropic parameters for layer-type and chain-like anisotropic crystals in Fig.5.3. The flections of the density of states at critical points are smeared out by broadening effect.

5.3 Energy Parameter Modulation and Electrooptical Spectra in Anisotropic Crystals

In this section, we calculate the spectra of energy parameter modulation and electrooptical signals for layer-type and chain-like anisotropic crystals from the real and imaginary parts of dielectric constants, and discuss the behavior of the variation of the spectra among 1-, 2- and 3-dimensional crystal with anisotropic parameter r. In energy parameter modulation the signals can be expressed as the linear combination of the differentiated spectra of the imaginary and real part of complex dielectric constant as known from the discussion in chapter 2. Some relationships between energy parameter modulation spectra near critical point exist as mentioned in chapter 4, and so all the energy parameter modulation spectra are called in our minds

immediately, if only the differentiated spectra of $\varepsilon_1(\omega)$ and $\varepsilon_2(\omega)$ by photon energy is calculated. In electrooptical effect, the spectra can be also obtained with help of the third derivatives of dielectric constant as derived by Aspnes.[10] According to this third derivative theory, the electrooptical signal in the case of the large broadening is given by

$$\Delta\varepsilon(\omega,\Gamma) = \frac{1}{3E^2}(\hbar\Omega\frac{\partial}{\partial E})^3 \; E^2 \; \varepsilon(\omega,\Gamma), \tag{5.17}$$

where

$$(\hbar\Omega)^3 = \frac{1}{8} e^2 \; (\mathbf{E}\cdot\nabla_k)^2 \; E(k)$$

$$= \frac{e^2 E^2 \hbar^2}{8\mu}$$

and E is electric field. This simple relation between the electrooptical signal and the unperturbed dielectric constant is justified in the case that broadening factor is much larger than the characteristic electrooptical energy. When effective mass has no energy dependence, this relation may be more simplified as follows,

$$\Delta\varepsilon(\omega,\Gamma) = \frac{(\hbar\Omega)^3}{3}\frac{\partial^3}{\partial E^3}\varepsilon(\omega,\Gamma). \tag{5.18}$$

In these considerations, the spectra of energy parameter modulation and electrooptical effect for anisotropic crystals can be represented by the first and third derivatives of complex dielectric

constant. E^2 hardly affects the spectra of $\Delta\varepsilon(\omega,\Gamma)$ near critical point and therefore that component is neglected in the differentiation. The assumption of constant reduced mass in the direction of electric field is justified by the fact that electric field applied on sample is transverse to z-axis for layer-type crystal and parallel to z-axis for chain-like crystal.

The real and imaginary parts of the first and third derivatives of complex dielectric constants are drawn for some layer-type anisotropic crystals in Fig.5.4 and 5.5, and for some chain-like anisotropic crystals in Fig.5.6 and 5.7. In the 2-dimensional spectra the spectral behavior near critical point justly resembles the differential spectra calculated in the last section where the spectra near critical point are degenerate. As the interaction between layers, that is, anisotropic parameter r, increases, the differential signal near 2-dimensional M_0 and M_2 critical point is separated into two parts.[11] The one goes far from the former energy position and gradually forms the spectra near 3-dimensional M_0 and M_3 critical point with increasing r. The others move to the former 2-dimensional M_1 critical point in energy position, incorporate with the former doubly degenerate one at the former M_1 critical point and gradually form the one near 3-dimensional M_1 and M_2 critical point triply degenerated. The bottom spectra in Fig.5.4 and 5.5 are the one for simple cubic crystal. In Fig.5.6 and 5.7 the upper spectra are 1-dimensional ones and the spectral behavior near critical point justly resembles

the differential spectra calculated in the last chapter, which is triply degenerated. As the interaction between the chains, that is anisotropic parameter r, increases, the differential spectra located near the former 1-dimensional M_0 and M_1 critical point are separated into three parts.[12] The one goes far from the former energy position and gradually forms the one near 3-dimensional M_0 and M_3 critical point. The another at M_1 critical point rests at the same position, incorporates with the one at M_2 critical point separated from the former 1-dimensional M_1 critical point and gradually forms the one near M_1 critical point similar to the one near 3-dimensional critical point calculated in the last section. The other in M_2 critical point incorporates with the doubly degenerate one located at the former 1-dimensional M_1 critical point and gradually forms the triply degenerate one near 3-dimensional M_2 critical point similar to the one calculated in the last chapter.

Electrooptical signals are proportional to the third derivatives of dielectric constant multiplied by $(\hbar\Omega)^3$ under the condition of the constant effective mass in the direction of electric field. When electric field is in the direction of the positive mass, electrooptical signals are proportional to $\frac{d^3\varepsilon}{d\omega^3}$ in Fig.5.5 and 5.7. But when electric field is in the direction of the negative mass, they are proportional to $-\frac{d^3\varepsilon}{d\omega^3}$. These considerations are complicated near the energy region in which two types of critical points do interfere each other, as shown in Fig.5.5

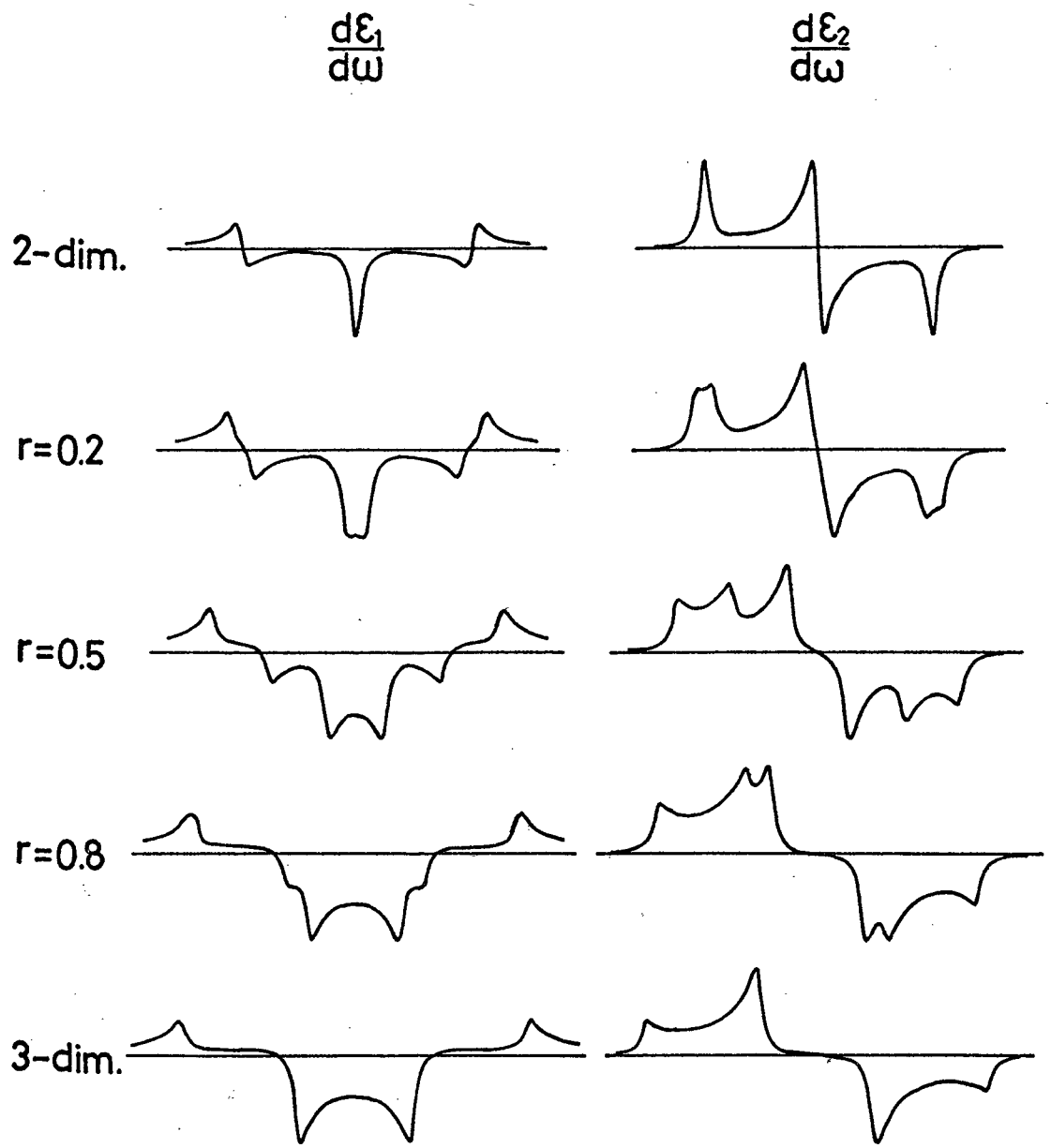

Fig.5.4 The real and imaginary parts of the first derivatives of complex dielectric constants for layer-type electronic structures with some anisotropic parameters.

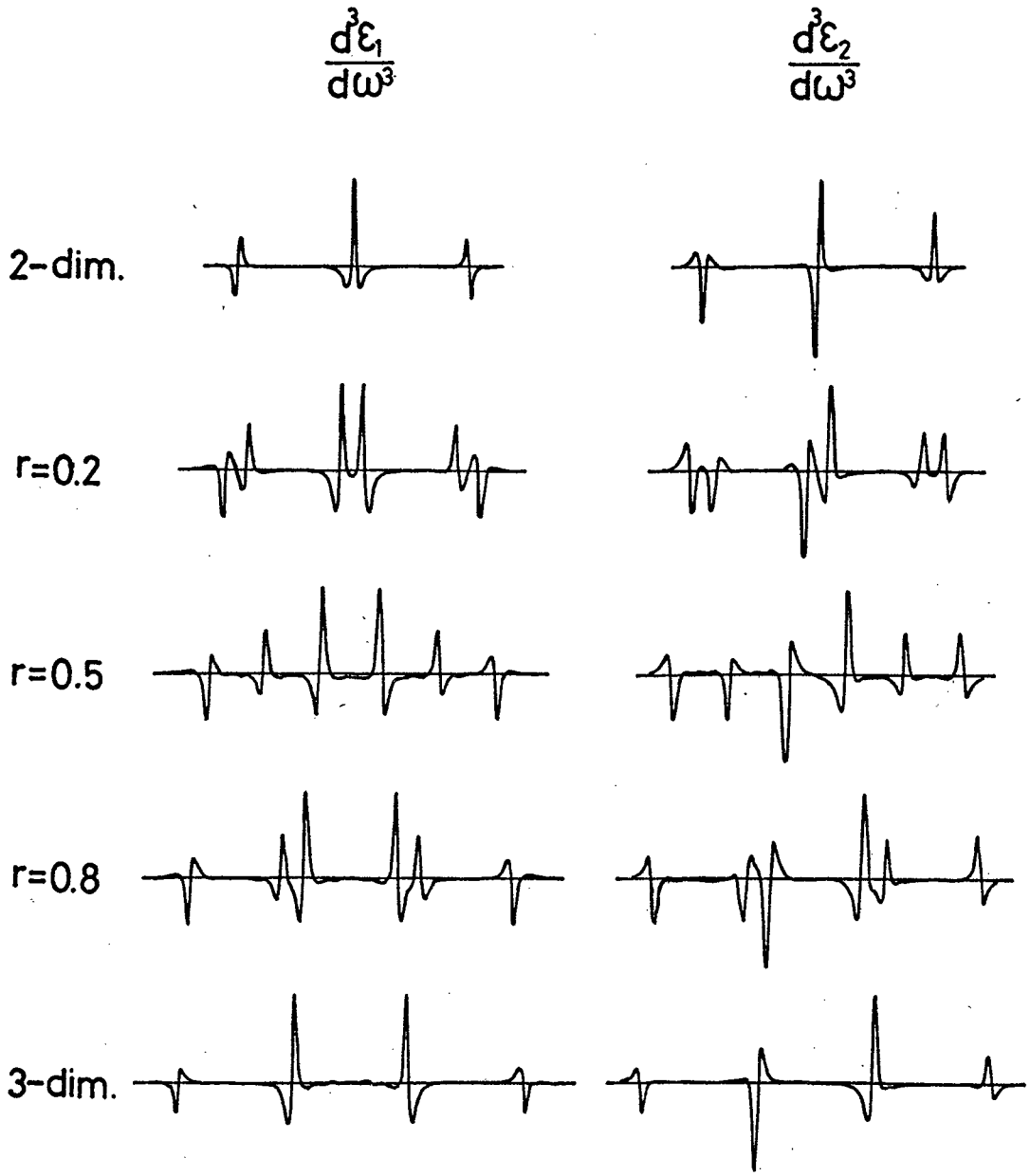

Fig.5.5 The real and imaginary parts of the third derivatives of complex dielectric constants for layer-type electronic structures with some anisotropic parameters.

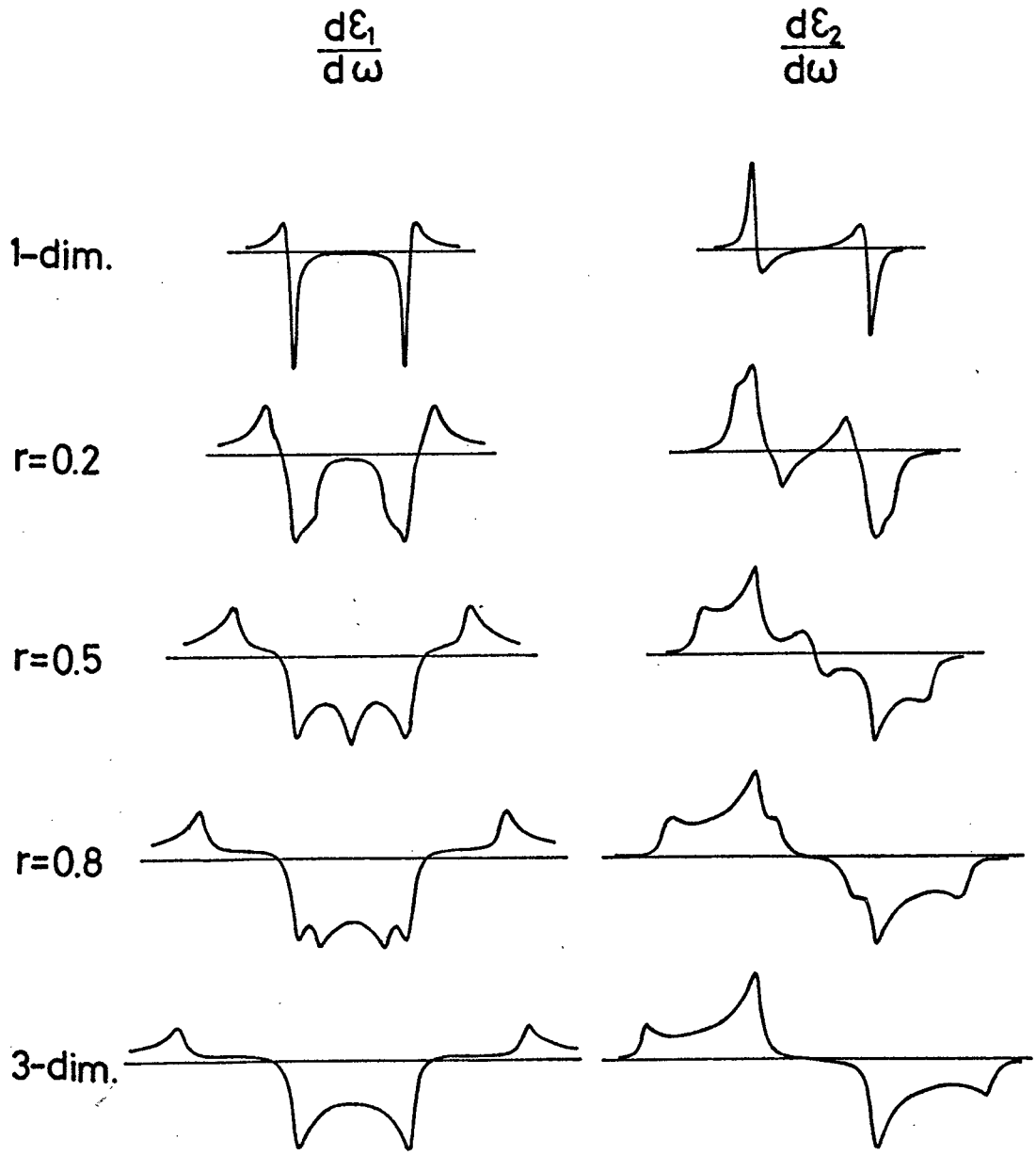

Fig.5.6 The real and imaginary parts of the first derivatives of complex dielectric constants for chain-like electronic structures with some anisotropic parameters.

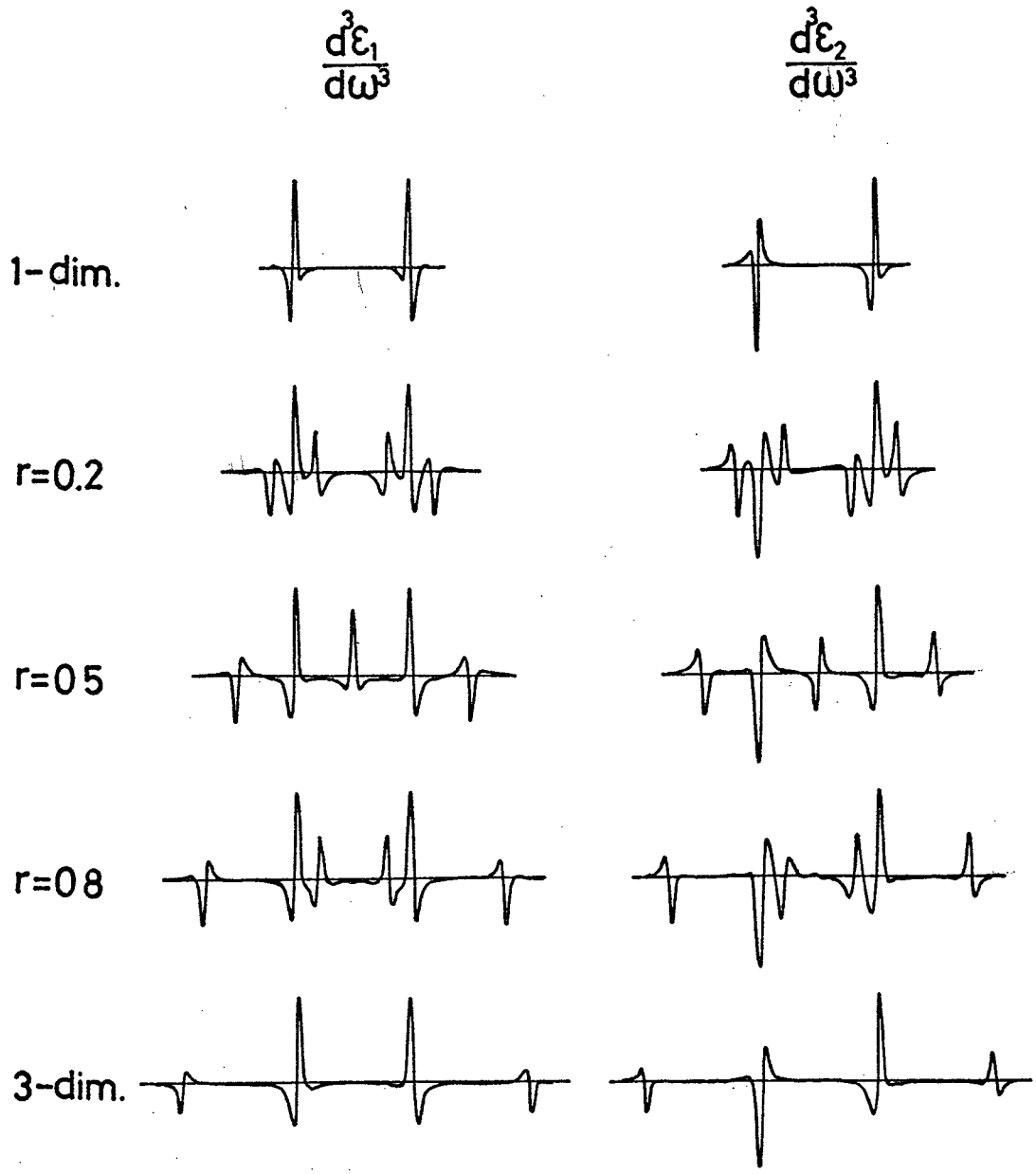

Fig.5.7 The real and imaginary parts of the third derivatives of complex dielectric constants for chain-like electronic structures with some anisotropic parameters.

and 5.7. However, in the case of electric field perpendicular to z-axis in layer-type crystal the relation mentioned above is kept a good approximation between electrooptical spectra and the third derivative of dielectric constant because of the invariance of the effective mass in the field direction. In chain-like crystals, for the good approximation the electric field must direct to z-axis.

5.4 Summary

In this section, energy parameter modulation and electro-optical signals were given in the intermediate anisotropic crystals. The density of states functions for the anisotropic crystals were calculated by assuming that the electronic band energy $E(k)=E_0-E_1(\cos k_x + q \cos k_y + r \cos k_z)$, where q and r are continuous anisotropic parameters. The complex dielectric constants with lifetime broadening are obtained by the convolution integral of density of states with Lorentzian type function and its dispersive line. From these calculations, variations of density of states function with changing crystal symmetry from one- or two- to three-dimensional crystal are represented and examined. Third derivatives of dielectric spectra with a broadening factor, which can be compared to electrooptical spectra from Aspnes' theory, are calculated as a function of continuous anisotropic parameter. The same kinds of calculations are extended to the other energy parameter modulated dielectric function. Change of the spectral responce with anisotropic parameters is also examined.

References

1. G. Harbeke, in *The Optical Properties of Solids*, Ed. by J. Tauc (Academic Press, New York, 1966) 90ff.
2. D. V. Chepur, D. M. Bercha, I. D. Tury and V. Yu. Slivka, Phys. Stat. Sol. 30, 461 (1968).
3. D. E. Aspnes and J. E. Rowe, the Proceedings of the 10th International Conference of the Physics of Semiconductors, (1970), 422ff.
4. R. Jellito, J. Phys. Chem. Solids 30, 609 (1969).
5. H. I. Ralph, Solid State Comm., 3, 303 (1965).
6. M. Shinada and S. Sugano, J. Phys. Soc. Japan 21, 1936 (1966).
7. O. Akimoto and H. Hasegawa, J. Phys. Soc. Japan 22, 181 (1967).
8. K. Nakao, J. Phys. Soc. Japan, 25, 1343 (1968).
9. P. F. Byrd and M. D. Friedman, in *Handbook of Elliptic Integrals for Engineers and Physicists* (Springer-Verag, Berlin, 1954)
10. D. E. Aspnes and J. E. Rowe, Phys. Rev. B 5, 4022 (1972).
11. M. Okuyama, T. Nishino and Y. Hamakawa (to be published).
12. M. Okuyama, T. Nishino and Y. Hamakawa (to be published in J. Phys. Soc. Japan).

6. CONCLUSIONS

Broadening effects of differential energy spectra in various energy parameter modulation have been investigated. Calculations were made for one-, two- and three-dimensional crystals on various types of critical points. Derivations and considerations on broadened energy spectra in modulation spectroscopy have been discussed by two separate categories, i.e., electric field modulation and other energy parameter modulation. The main results worked out in this thesis work are enumerated as following.

1) In electrooptical effect, two broadening factors due to thermal and electric field effects were taken into account as the Lorentzian convolutions in the electrooptical functions for three-dimensional crystal.
2) Variations of the amplitudes in the field induced changes of complex dielectric constants, $\Delta\varepsilon_1$ and $\Delta\varepsilon_2$, with the amount of broadening factors Γ_T and Γ_E were presented for a series of certain realistic parameters.
3) Parametric changes in the broadened electrooptical spectra with the amount of broadening factors were also discussed.
4) Calculated electrooptical functions enabled us to compare quantitatively with the spectra measured in the electrooptical experiments, and considerable agreements between the theory and experimental result were obtained.
5) One- and two-dimensional electrooptical functions with

broadening were also calculated. Until now, no typical experimental results have been reported, but the calculated broadened electrooptical functions on these anisotropic crystals would be a useful theoretical background for experimental work.

6) A generalized expression of broadened complex dielectric functions near one-, two- and three-dimensional critical points has been demonstrated as functions of parameters of photon energy $\hbar\omega$, critical point energy $\hbar\omega_g$ and broadening factor Γ.

7) A systematic relationship has been found in differential dielectric functions modulated with energy parameters of ω, ω_g and Γ. By using the relationship, the line shapes of the modulated spectra for any dimensional critical point can be easily figured from a differential function.

8) Density of states functions for anisotropic crystals were calculated by assuming that the electronic band energy $E(k) = E_0 - E_1(\cos k_x + q \cos k_y + r \cos k_z)$, where q and r are continuous anisotropic parameters.

9) Complex dielectric constants with lifetime broadening are obtained by the convolution integral of density of states with Lorentzian type function and its dispersive line.

10) Variations of density of states functions with changing crystal symmetry from one- or two- to three-dimensional crystal are represented and examined.

11) Third derivatives of dielectric spectra with a broadening factor, which can be compared to electrooptical spectra,were calculated as a function of continuous anisotropic parameter. The same kinds of calculations were extended to the other energy parameter modulated dielectric function. Change of the spectral responce with anisotropic parameters is also examined.

VITA

Masanori Okuyama was born in Kawachinagano, Osaka, Japan on March 4, 1946. He graduated from Sumiyoshi Senior High School, Sumiyoshi, Osaka in March 1964 and entered Osaka University, Toyonaka, Osaka in April of that year. He graduated from Osaka University in March of 1968 and entered the Graduate School in April of that year. While at Osaka University, he became a member of the Physical Society of Japan. He received his Master of Engineering degree in Electrical Engineering in March, 1970 from Osaka University.